Evaluation of Field-Collected Drifter and In Situ Fluorescence Data Measuring Subsurface Dye Plume Advection/Dispersion and Comparisons to High-Frequency Radar-Observation System Data for Dispersed Oil Transport Modeling

APPENDIX B – PHOTOGRAPHIC DATA

A Final Report Submitted to

The Coastal Response Research Center

Submitted by:

Dr. James R. Payne
Payne Environmental Consultants, Incorporated
1991 Village Park Way, Suite 206B
Encinitas, CA 92024

Additional Investigators:

Dr. Deborah French-McCay, Chris Mueller, Kathy Jayko,
Brooke Longval, and Melanie Schroeder
Applied Science Associates, Inc.
Narragansett, Rhode Island

Dr. Eric Terrill, Melissa Carter, Mark Otero,
Sung Yong Kim, William Middleton, and Andy Chen
Scripps Institution of Oceanography
La Jolla, California

Dr. Walter Nordhausen, Robin Lewis, Mark Lampinen, and Thomas Evans
CA Department of Fish and Game Office of Spill Prevention and Response
San Diego, California

Dr. Carter Ohlmann
University of California Santa Barbara
Santa Barbara, California

Project Period: January 2006 – September 2007
Submission Date: May 11, 2007
Revised:

This project was funded by a grant from NOAA/UNH Coastal Response Research Center.
NOAA Grant Number(s): NA04NOS4190063 (CFDA No. 11-419). Project Number: 06-084

Table of Contents

List of Figures

List of Tables

Appendix B. Photographic Data

Observations from the California Department of Fish and Game fixed-wing aircraft (twin engine, Partenavia) were used to orient the sampling effort and photo document the movements of dye relative to the drifters. In the first field experiment completed in November 2005, the pilot and two observers were able to record the deployment and drift of the dye and drifters, and take multiple digital pictures. Photos were made using the visual light spectrum from a hand-held digital camera, as well as a multi spectral camera (operated by Ocean Imaging, Inc.) fixed to the plane and pointing downward through a viewing window. During all subsequent flights a Nikon digital camera fixed to the plane and pointing downward through the viewing window was used.

This appendix contains the photographic image data, including detailed methods, example images, and summaries of the dimensions of the dye estimated from the images. All the images and derived products (such as shape files) were provided electronically and are available on an ftp site (ftp://ftp.mpl.ucsd.edu/pub/CORDC/outgoing/OSPR). Section B.1 describes the methods, and Sections B.2 to B.9 contain data collected for each of the experimental dates.

B.1 Approach and Methods for Image Processing

B.1.1 Dye Plume Shape Extraction Methods and Georeferencing

The aerial photographs taken during the dye experiments were processed to determine the size, position, and orientation of the dye plume over the course of each experiment. Ideally, the camera captured a variety of information from the GPS unit on the aircraft and digitally appended the information to each photograph. Thus, each image was digitally stamped with the time, location (latitude-longitude), altitude, and heading at the time the picture was taken. This information allowed each image to be georeferenced with a fairly good degree of accuracy.

Unfortunately, during several of the experiments, one or more pieces of information were not collected on a per-image basis (reference Error Section). For these experiments, various "workarounds" had to be developed to obtain the necessary information. For example, in the case of the March 21st and 22nd experiments, none of the recorded information was digitally appended to the photographs. Instead, the information was transcribed to an excel spreadsheet after the experiment was concluded Additionally, heading information recorded by the aircraft during the March experiments was not transcribed and was instead captured from the hand-written log kept by scientists on the aircraft (March 21st) or calculated from the image locations (March 22nd) . This process likely introduced some error and is likely responsible for the higher degree of "jumpiness" observed in the March experiments (see Section B.3). However, the dimensions (area, down-wind axis and cross-wind axis) are the basic data used for analysis of dye diffusion rates, and these are not affected by the absolute position.

Once the necessary information was assembled, the single position (latitude-longitude) correlated to each image was used to georeference the image. The following procedure was used for all experiments:

Note: Georeferencing for the experiments off San Diego was performed using the UTM Zone 11N coordinate system. Georeferencing for the Safe Seas experiment off San Francisco used the UTM Zone 10N coordinate system. The UTM coordinates provided more accuracy during calculations and transformations, as latitude/longitude conversions were avoided.

Pre-Processing:

**The following was performed using a custom application which ingested the name, center longitude coordinate, center latitude coordinate, field of view, and heading information and produced a ".shift" file for each image

1. Given the altitude (*h*) and field of view (*f*) for the camera, the following calculation can be used to determine the swath width (*sw*) of the image. The assumption in this equation is that the camera is exactly perpendicular to the ocean surface.

$$sw = 2 * h * \tan((\frac{\pi}{180}) * (\frac{f}{2}))$$

2. The swath width can then be divided by the number of pixels in the horizontal (in this case 3008) to calculate the width of a single pixel (*p*).
3. This pixel size can then be used to calculate the ground distance in the vertical dimension.
4. Using the assumption that the location recorded by the plane represents the center of the corresponding image, and the ground width and height calculated as above, the positions of the four corners of the image can be calculated.
5. The results of this calculation, along with the corresponding heading for the image, were exported to text files (one for each image).

Image Georeferencing:

Georeferencing was performed using a custom utility for ESRI's ArcMap Geographic Information System [GIS] software. The utility ingested the .shift files and the original .jpg images and produced a georeferenced .tif file for each image. The utility first moved and resized the image based on the transformation information in the .shift file and then used the heading information to rotate the image to the proper orientation.

Image Post-Processing:

Once the images were georeferenced, image processing software (ENVI 4.3) was used to extract the dye plume from each image and create a "shape file" (i.e., a trace of the outline, in the commonly used format employed by ESRI's ArcMap Geographic Information System [GIS] software) representing the extent of the dye plume. The software performed a "band math" operation to create a single band image, which showed the dye in sharp contrast to the

surrounding water. The equation for the band math operation (where b_R is the calculated band and b_r, b_g, and b_b are the red, green and blue bands respectively) was:

$$b_R = b_g - \left(\frac{(b_r + b_g + b_b)}{3} \right)$$

This intermediate image was then "classified" by the software to extract the initial dye shape file. The shape file was then post-processed to remove noise and calculate the area, cross-wind axis, down-wind axis, and centroid (spatial center) for the plume over the course of the experiment.

Figure B.1-1 below shows the workflow for the Image-to-Shapefile process.

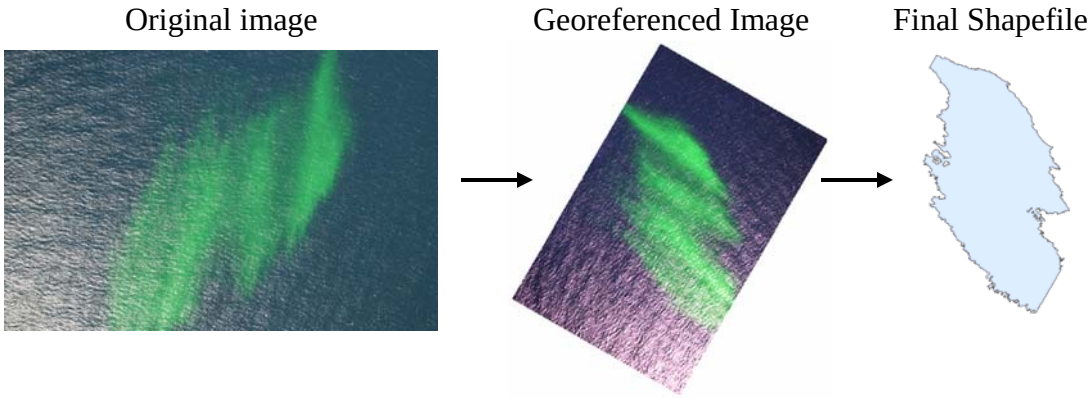

Figure B.1-1. Aerial photograph processing steps to create shape files.

B.1.2 Dye Intensity Processing

The ENVI Software was again used to process the images to extract relative dye intensity information. The same "band math" operation was performed on the georeferenced images and then the pixel values were "binned" into ten (10) intensity levels. The levels were based on the range of values from the first (earliest) image of a given day. The bins determined from the initial image were then used to process all of the images for a given day. This allows direct comparison of the images during the course of a day. The result was an image of the plume that was categorized by the intensity of the dye. The workflow is shown in Figure B.1-2. The "bin" value of each pixel in the intensity image was then exported to an XYZ file (longitude, latitude, intensity) for use in the dispersion analysis.

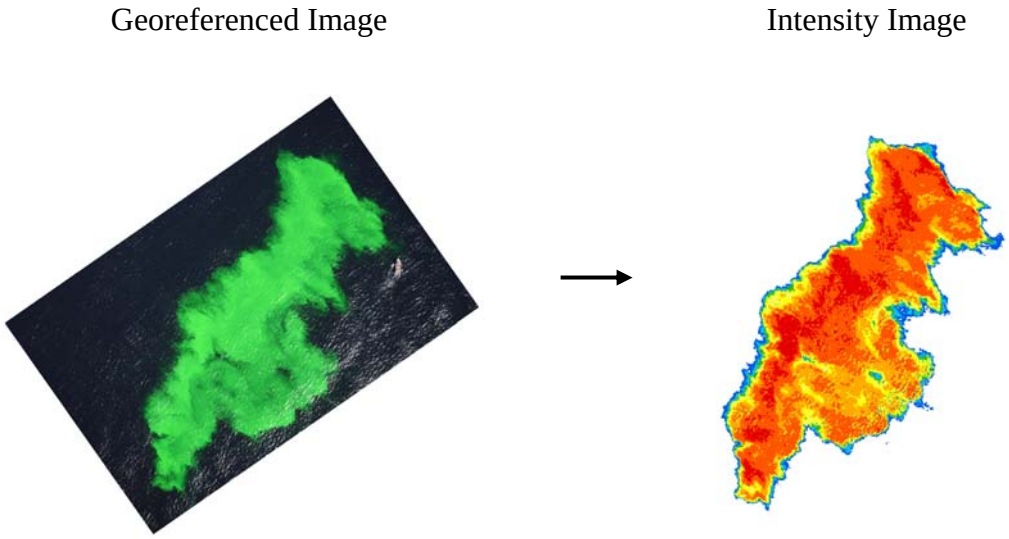

Figure B.1-2. Aerial photograph processing steps to create binned intensity images and data files.

B.1.3 Dye Image Files

Table B.1-1 contains the naming convention for image files (provided electronically) for experiments on 21-22 March 2006, 21-22 June 2006, and 1-2 November 2006. All GIS shape files are projected in GCS-WGS-'84 latitude/longitude coordinate system. Image files for the experiment performed on 8 November 2005 do not follow the same naming convention. The original *.tif images were provided by Ocean Imaging and converted to shape files by ASA (see section B.2 for list of files). Note: # = image number.

Table B.1-1. Naming convention for image files for experiments on 21-22 March 2006, 21-22 June 2006, and 1-2 November 2006.

Image File Type	File name format	Description
*.jpg	DSC_#.jpg	Original aerial image of plume
*.tif	DSC_ #.tif	Georeferenced image of plume
*.shp	(Date)_Final_shp.shp	GIS shape file of all plume images
*.shp	filt_Class_#_shp.shp	GIS shape file of individual image

B.1.4 Langmuir Cell Spacing from Georeferenced *.tif files

Four or five images were chosen from each date (March 21, 22 and November 1, 2) based on completeness of the plume in the picture and visibility of the Langmuir cells. Photos from the June 2006 experiments were not suitable for this analysis because of glare on June 21 and the necessity to composite images for June 22 due to the low ceiling and altitude used for photography. Images were spaced as equally in time as possible from the first image where Langmuir circulation was visible until the end of the experiment. In ArcMap, Langmuir cells were identified and labeled with lines at the divergence zones (upwellings) of each cell, visualized as dark streaks separating areas of higher dye intensity. Heading was measured relative to a vertical line indicating north. Distances between the cells were measured using the distance tool in ArcMap, at approximately the mid point of each drawn line. Major cells were identified with red lines, while minor cells were identified with blue lines (see example, Figure B.1-3). Results for measured images are provided in these date's results Sections B.3, B.4, B.7 and B.8.

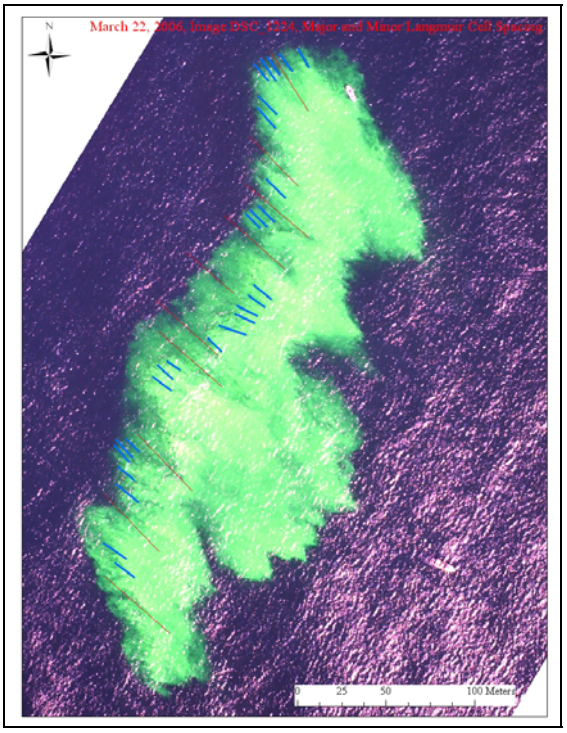

Figure B.1-3. Example of Langmuir cell spacing (10:43 AM, 22 March, 2006, image 1224). Major cells are identified with red lines, while minor cells were identified with blue lines.

B.1.5 Sources of Georeferencing Error

Typically, image orthorectification is done using specialized imaging equipment which records the precise location, time, deviation from perpendicular, altitude, and a variety of other variables. All of these measurements go into calculating the precise location, orientation, and scale of the orthorectified image. Additionally, orthorectified images are usually 'ground truthed' by crosschecking features visible in the image with known locations for those features (obtained by GPS).

In this series of experiments, such equipment and techniques could not be employed. Instead, the position, altitude, and heading of the aircraft carrying the digital camera was used to orthorectify the images. This method incurs a good deal of error, but still provides a fairly accurate approximation of the true location, scale, and orientation of the images.

All of the images incurred a certain amount of error due to the limitations of the collection method. The magnitude of all general error sources is dependant on the altitude of the plane when the image was captured. The error sources general to all experiments include:

1. Deviation of camera orientation from perpendicular to ground. Different for every image.
    a. This is dependant on the pitch and yaw of the plane, as well as the altitude at the time a particular image was taken.
    b. The approximate magnitude of this error varies from centimeters to kilometers.
2. Location of dye plume within the image frame.
    a. This is dependant on how far off center the dye is, the rotation of the image, and the altitude of the plane at the time the image was taken.
    b. The approximate magnitude of this error is generally in the 0 – 100's of meters range, but could potentially be kilometers if the altitude is large enough.

There were sources of errors specific to various experiments and are outlined and explained in each date's results section (B.2 – B.8).

B.2 Results of November 8, 2005 Experiment

B.2.1 Movement and Spreading of Dye

The 8 November 2005 experiment began at 10:26 PST (18:26 UTC) and ended approximately 16:15 PST (00:15 UTC on 9 November). Figure B.2-1 contains four images of the dye plume at times early in the experiment, as interpreted from the aerial photographs. The CTD casts and corresponding times in Figure B.2-1 represent the dye plume movement for the rest of the experiment. (See also Appendix A.2, Figure A-1.) The drifters followed the same path as the dye (Figure B.2-2), but moved faster than the dye. The drifters ended up near the coast of Point Loma north of the dye at about 16:15 PST. Figure B.2-3 is a close-up of the four images of the dye plume. Figures B.2-4 to B.2-8 based on the four photographs show shape files of these images (provided by Ocean Imaging). The ratio image (Figure B.2-8) indicates the intensity of the dye, integrated over depth, captured by the image. Table B.2-1 lists the file names for the four images.

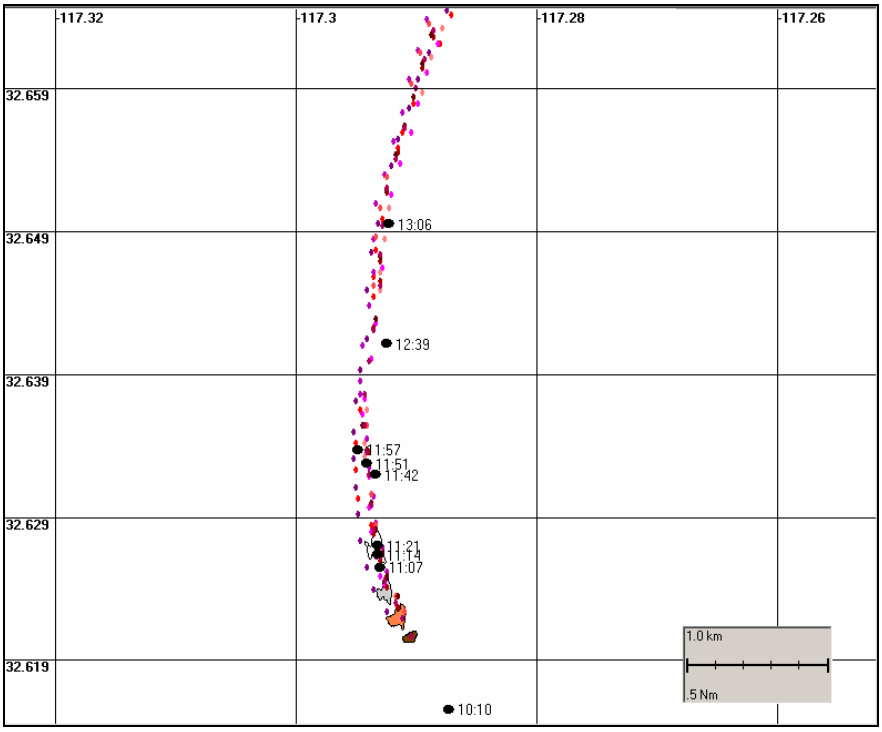

Figure B.2-1. Locations of the dye over time in the 8 November 2005 experiment, as interpreted from the aerial photographs. Waypoints of drifter movements (drogued at 1m) are indicated as diamonds. Circles and times indicate locations of the dye during CTD casts.

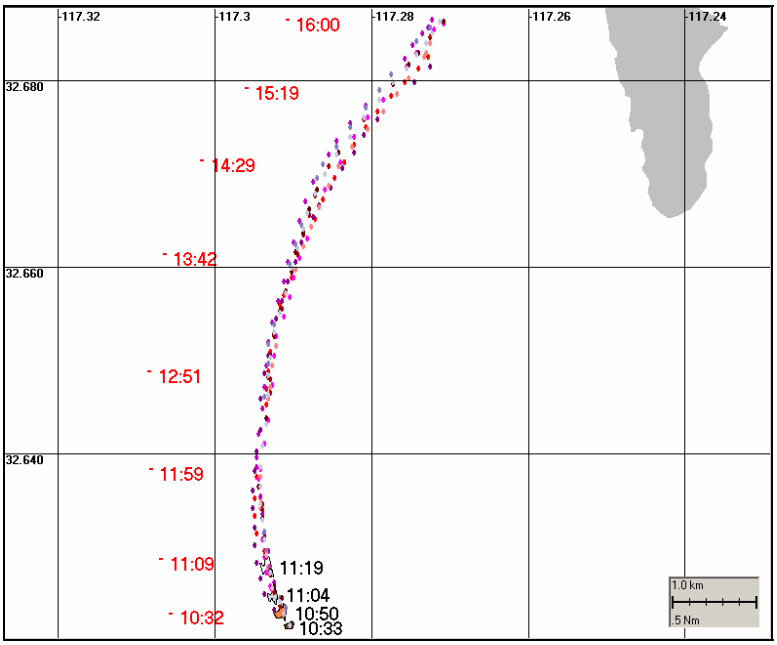

Figure B.2-2. Dye plume dimensions and movements over time, and drifter tracks represented by diamonds (all 1m deployment depth) for the 8 November 2005 experiment. Four images of dye plume are shown with corresponding times (black font). Corresponding times for drifter tracks (diamonds) are in red font.

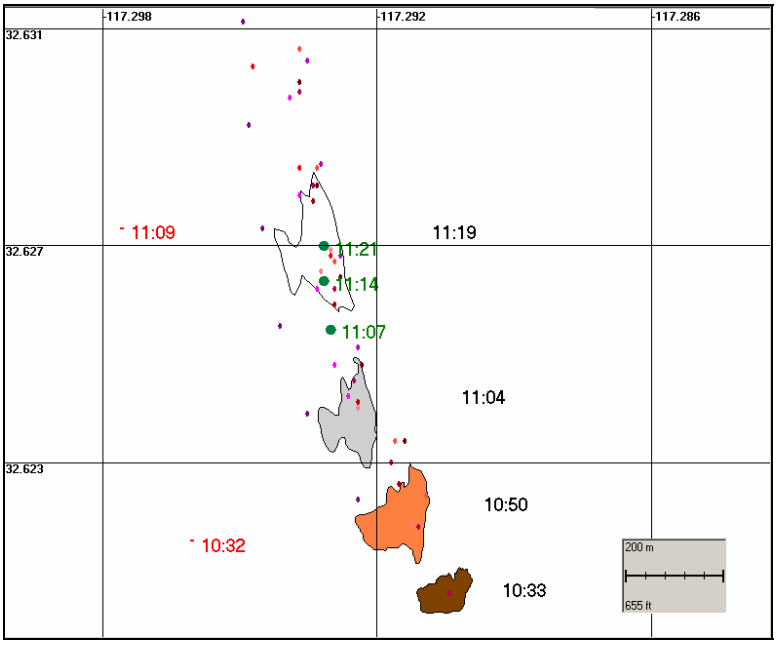

Figure B.2-3. Close up of dye plume dimensions and movements over time, and drifter tracks represented by diamonds (all 1m deployment depth) for the 8 November 2005 experiment. Four images of dye plume are shown with corresponding times (black font). Corresponding times for drifter tracks (diamonds) are in red font. Circles and times (green font) indicate locations of the dye during CTD casts.

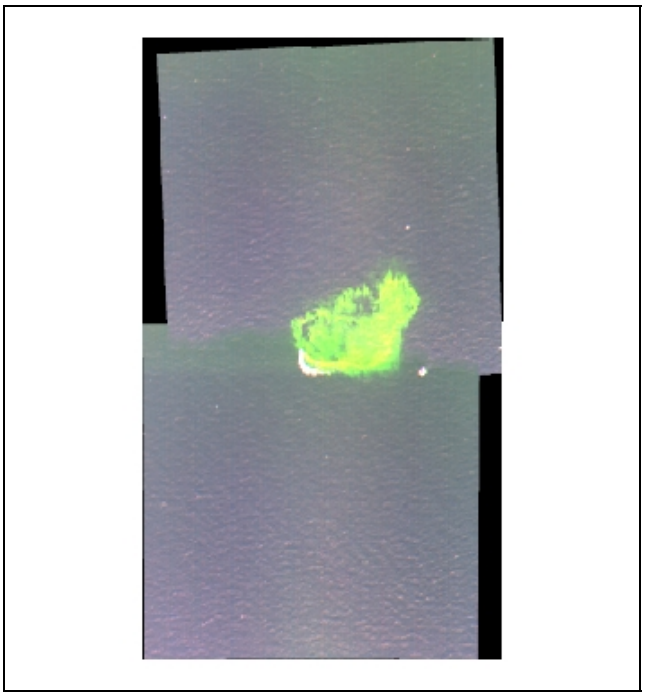

Figure B.2-4. Georectified *.tif images of dye plume (10:36 AM on 8 November 2005), provided by Ocean Imaging.

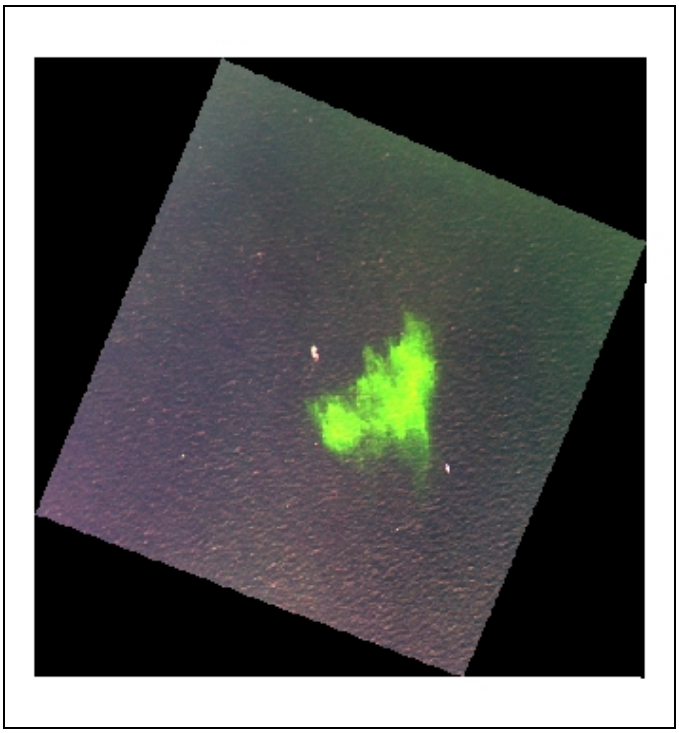

Figure B.2-5. Georectified *.tif images of dye plume (10:50 AM on 8 November 2005), provided by Ocean Imaging.

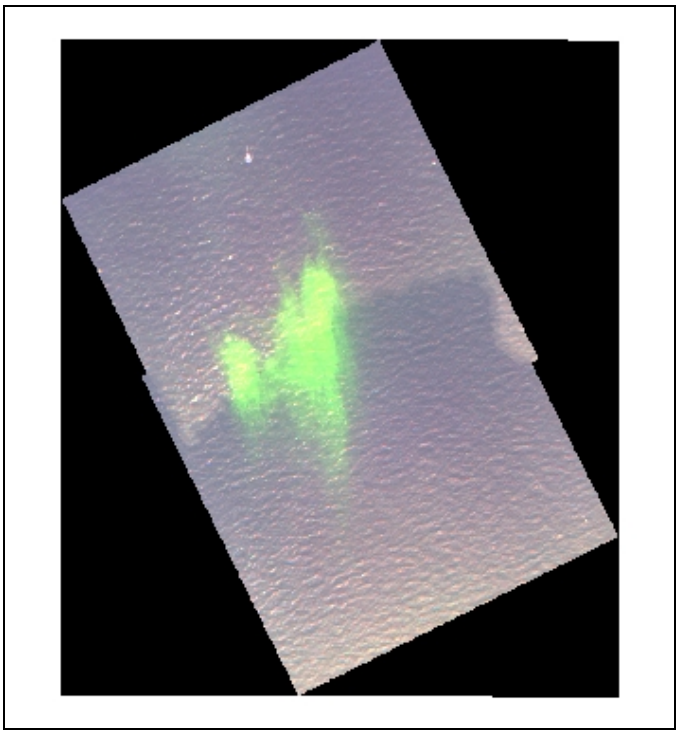

Figure B.2-6. Georectified *.tif images of dye plume (11:04 AM on 8 November 2005), provided by Ocean Imaging.

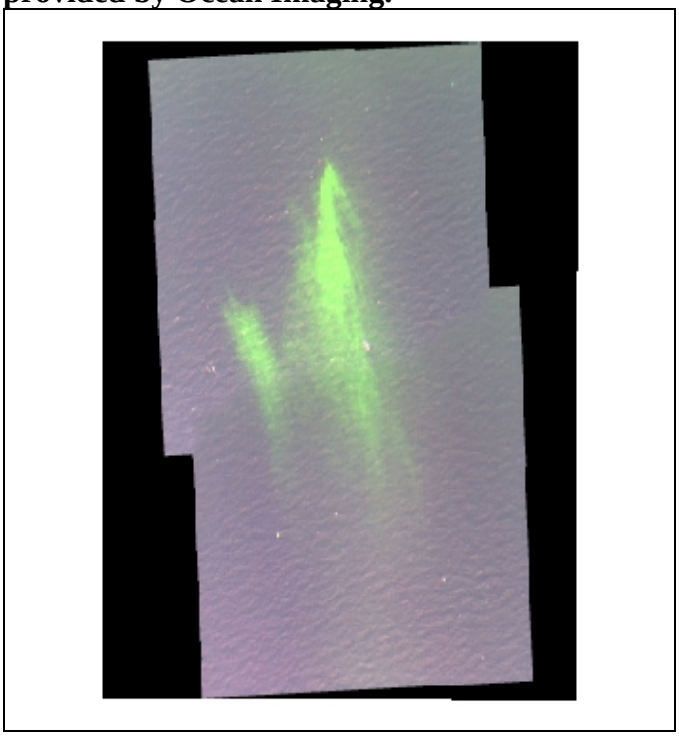

Figure B.2-7. Georectified *.tif images of dye plume (11:19 AM on 8 November 2005), provided by Ocean Imaging.

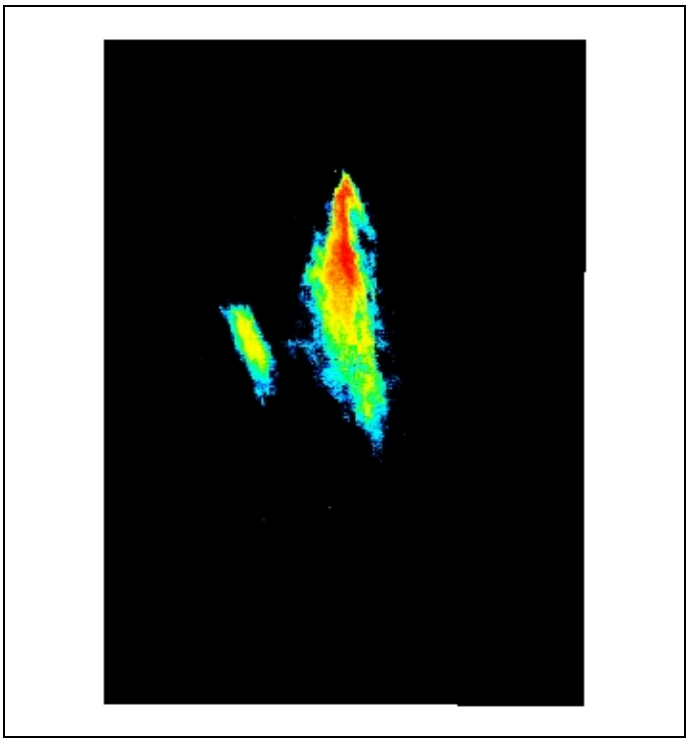

Figure B.2-8. Ratio image developed from georectified *.tif (11:19 AM on 8 November 2005), provided by Ocean Imaging.

Table B.2-1. Naming convention for image files for the 8 November 2005 experiment (provided electronically). All GIS shape files are projected in GCS-WGS-'84 latitude/longitude coordinate system. Original *tif files provided by Ocean Imaging. Note: # = image number.

Image File Type	File name format	Description
*.tif	dmsc_110805_#am_(ratio).tif	Georeferenced image of plume
*.shp	Nov8_#.shp	GIS shape file of individual image

B.2.2 Dimensions of Dye Over Time

Table B.2-2 lists the images used in the analysis of dye plume dimensions over time. The growth of the area, down-wind axis length and cross-wind axis length over time is plotted in Figures B.2-9 to B.2-11.

Table B.2-2. Data for all plume images on 8 November 2005.

Image #	Time (PST)	Down-wind axis (m)	Cross-wind axis (m)	Area (m^2)
1033	10:33AM	80.64	121.93	6,810
1050	10:50AM	158.14	182.14	15,612
1104	11:04AM	182.14	117.19	13,325
1119	11:19AM	225.26	128.70	21,239

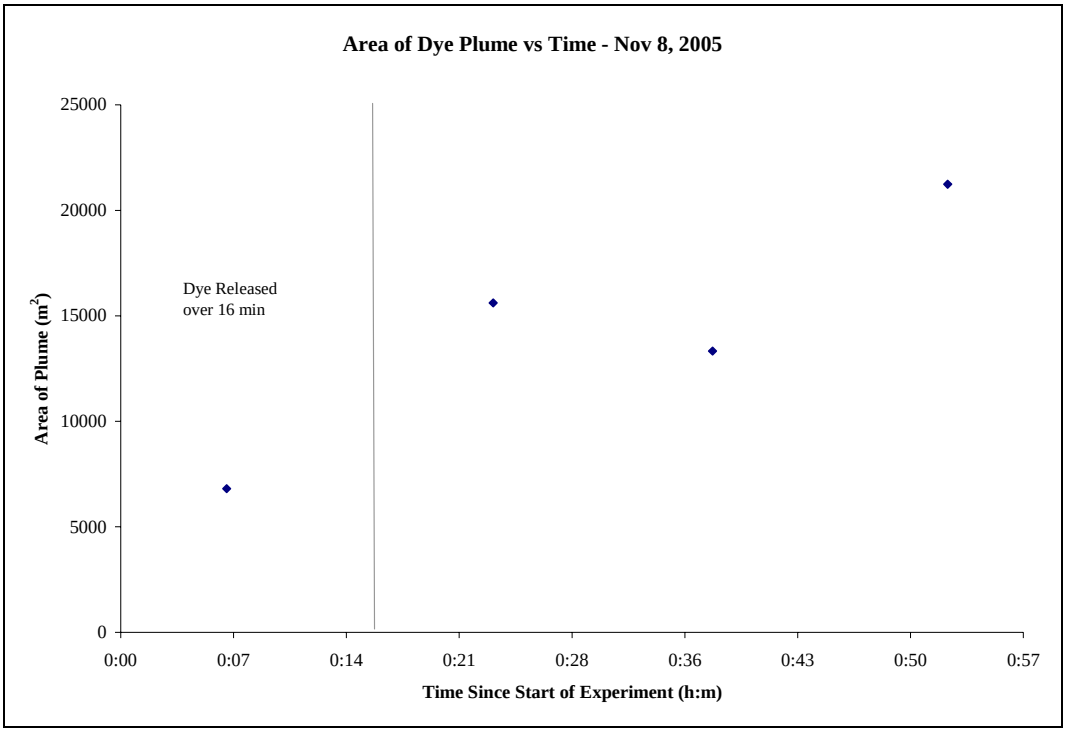

Figure B.2-9. Growth of the area of the plume, as measured from the images.

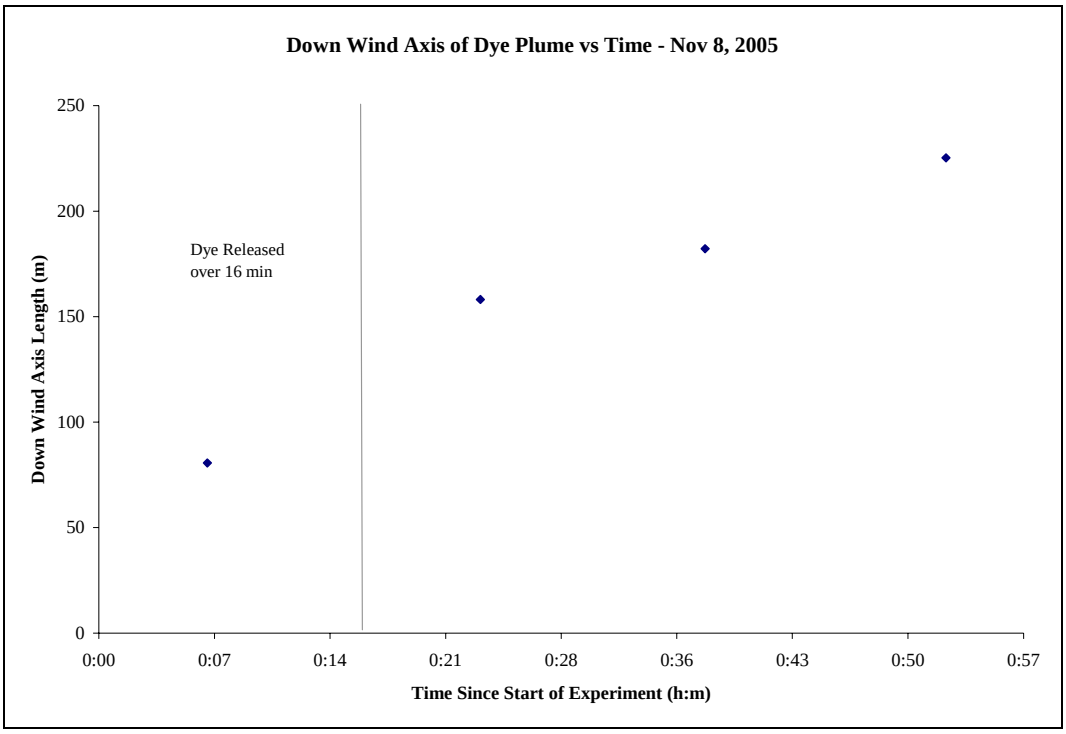

Figure B.2-10. Growth of the down-wind axis of the plume, as measured from the images.

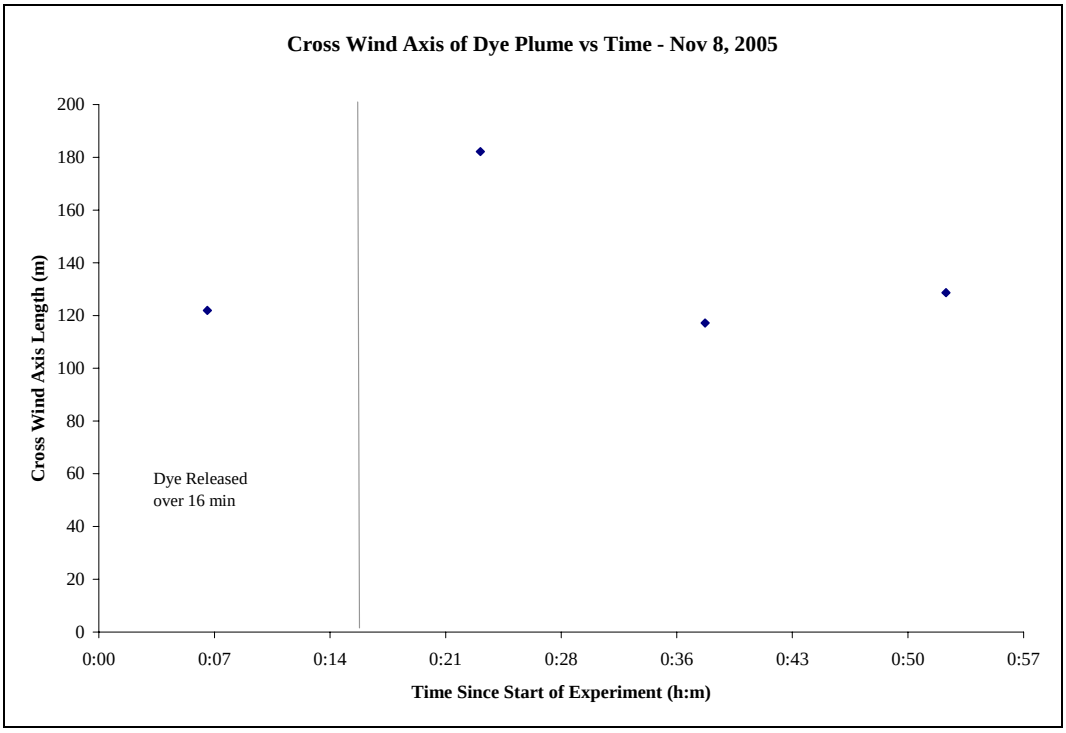

Figure B.2-11. Growth of the cross-wind axis of the plume, as measured from the images.

B.3 Results of March 21, 2006 Experiment

B.3.1 Movement and Spreading of Dye

The 21 March 2006 experiment began at 11:43 PST (19:43 UTC) and ended approximately 13:50 PST (22:50 UTC). The dye moved toward the south-southeast in this experiment. Figure B.3-1 contains a subset of images that show the locations of the dye over time, as interpreted from the aerial photographs. Some of these shapes appear to be displaced to the west. These outlined shapes represent a few of the images with major georeferencing errors (see section B.1.1 for description of sources of error general to all experiments.) Table B.3-1 lists the file names for the images with major georeferencing errors.

Sources of error specific to date:

- Headings on this date were not recorded digitally. Hand written heading information was tied to the other digital image information based on time. When there was no matching heading record for a given image, the previous heading was used.
- Positional information for the images was transcribed from the image headers in DMS form which were then converted to Decimal Degrees. Though the data were checked twice and some transcription errors caught, there is still the potential that transcription errors persisted and affected the locations of the images.

Figure B.3-1 contains images of the dye plume over the time of the experiment, overlaid with locations of drifters, as recorded by GPS waypoints. Figure B.3-2 contains the same images of the dye plume over the time, with the centroids of each plotted and labeled with the time of the image. Figures B.3-3 and B.3-4 show example georeferenced images. Figures B.3-3 and B.3-4 also show these images color coded by dye intensity (in arithmetically-scaled bins). Other images are available on the ftp site (see introduction on page 1 of Appendix B).

Table B.3-1. March 21, 2006 images with major georeferencing errors.

Image #	Time (PST)
1123	11:45AM
1124	11:47AM
1152	12:49PM
1153	12:53PM
1154	12:57PM
1171	1:26PM
1183	1:45PM
1184	1:48PM
1186	1:52PM
1187	1:54PM
1192	1:57PM
1194	2:00PM

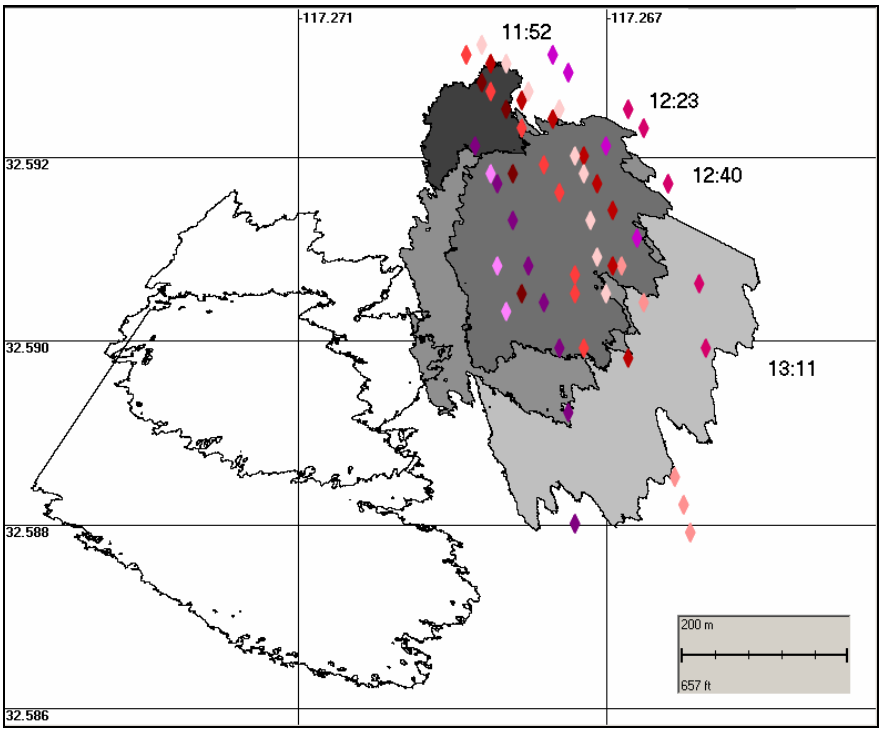

Figure B.3-1. Dye plume dimensions and movements over time, and drifter tracks represented by the diamonds (all 1m deployment depth) for the 21 March 2006 experiment. Examples of dye plume images with georeferencing errors are shown in outline only.

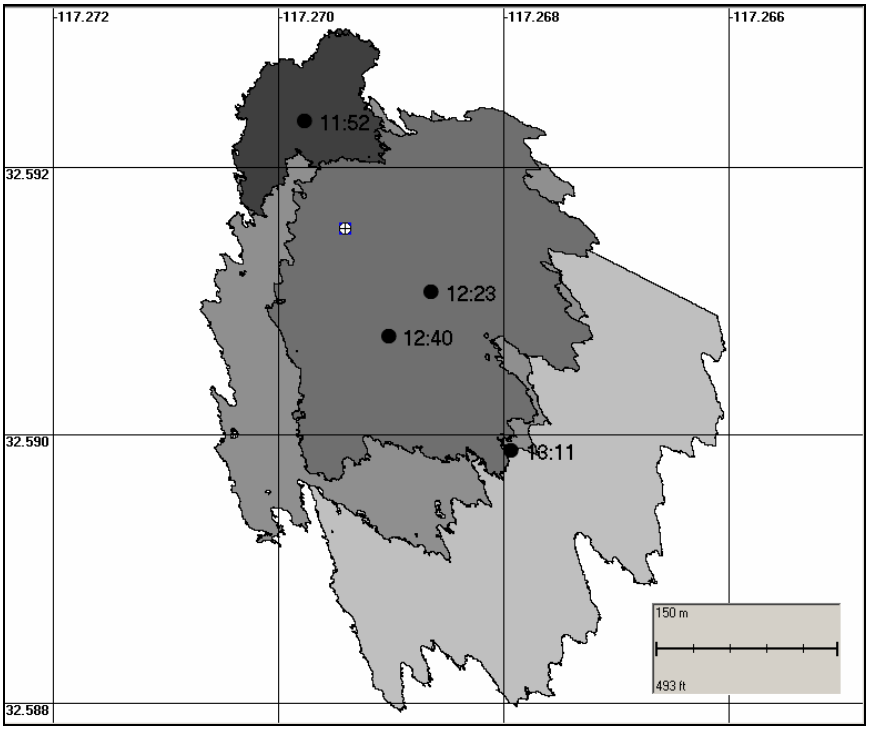

Figure B.3-2. Centroids of selected dye plume images and corresponding times for 21 March 2006 experiment.

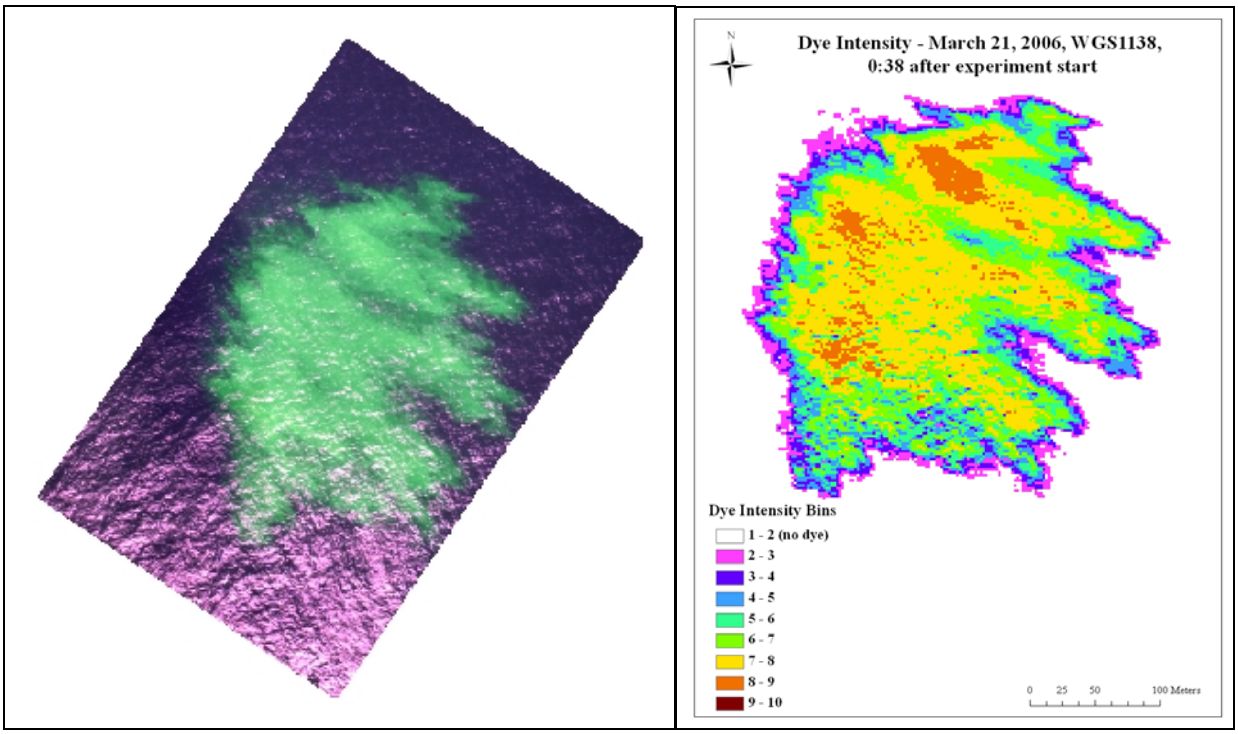

Figure B.3-3. Georectified *.tif and intensity binned (10bin) images of dye plume (image #1138, 12:23 PM on 21 March 2006).

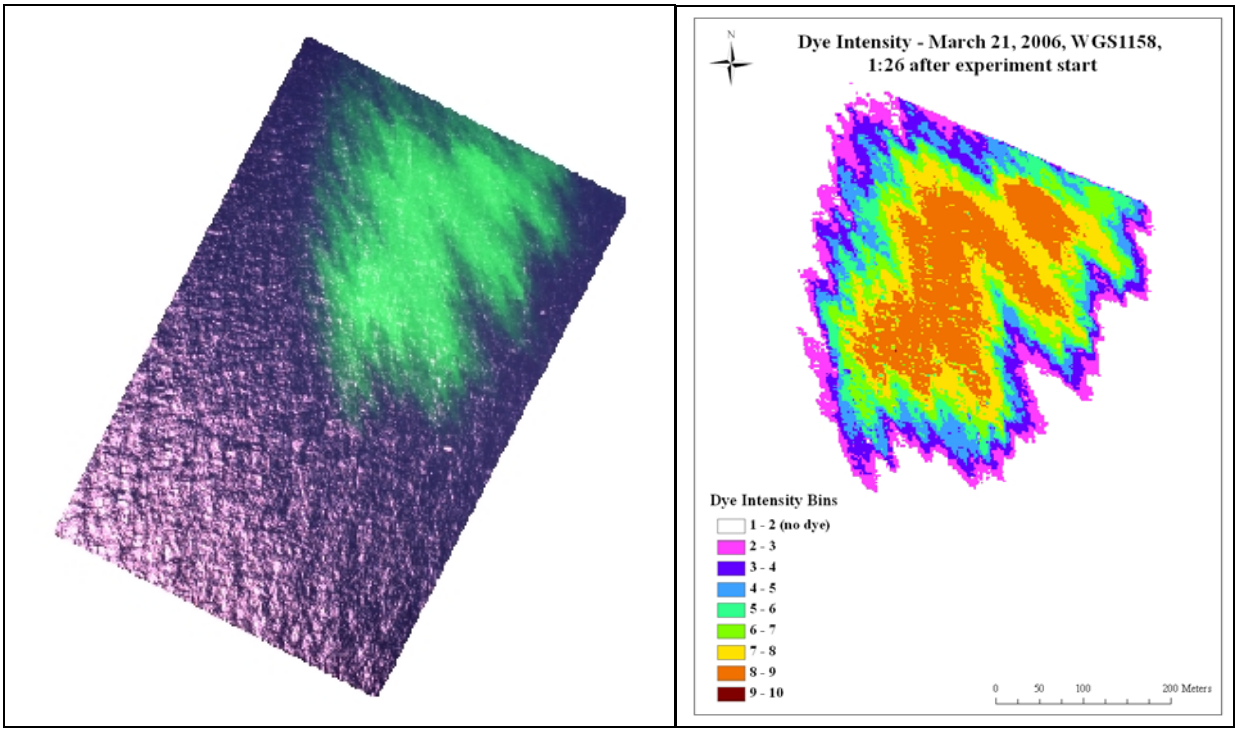

Figure B.3-4. Georectified *.tif and intensity binned (10bin) images of dye plume (image #1158 at 1:40 PM on 21 March 2006).

B.3.2 Dimensions of Dye Over Time

Table B.3-2 lists the images used in the analysis of dye plume dimensions over time. The growth of the area, down-wind axis length, and cross-wind axis length over time are plotted in Figures B.3-5 to B.3-7.

Table B.3-2. Data for plume images on 21 March 2006. Positions of centroids are approximate due to inaccuracy of dye image locations.

Image #	Time (PST)	Altitude (m)	Down-wind axis (m)	Cross-wind axis (m)	Area (m^2)	Centroid (x)	Centroid (y)
1133	12:10 PM	603	234	231	39,333	-117.26947	32.59092
1134	12:13 PM	588	241	255	42,258	-117.26883	32.59175
1138	12:23 PM	591	278	262	57,927	-117.26863	32.59106
1141	12:29 PM	756	303	299	69,527	-117.27004	32.59131
1142	12:32 PM	741	312	339	76,862	-117.27052	32.59048
1145	12:37 PM	751	315	358	78,506	-117.27068	32.59106
1147	12:40 PM	735	316	364	80,321	-117.26901	32.59072
1148	12:45 PM	771	335	382	89,385	-117.27202	32.58992
1152	12:49 PM	735	319	386	86,786	-117.25703	32.59027
1153	12:53 PM	737	309	372	77,580	-117.25349	32.59108
1154	12:57 PM	731	327	397	89,082	-117.25374	32.59045
1159	1:15 PM	895	448	341	101,243	-117.27016	32.59009
1162	1:18 PM	895	445	401	116,776	-117.27290	32.58974
1164	1:22 PM	917	420	459	133,943	-117.27178	32.58967
1171	1:26 PM	890	446	418	133,949	-117.25284	32.58920
1175	1:34 PM	1054	528	420	154,312	-117.27216	32.58871
1183	1:45 PM	1062	601	432	158,884	-117.27868	32.59040
1184	1:48 PM	1092	547	423	160,472	-117.28172	32.58955
1186	1:52 PM	1046	524	463	167,031	-117.28337	32.58900
1192	1:57 PM	1031	610	434	175,405	-117.28050	32.58953
1203	2:10 PM	1071	627	471	186,231	-117.27991	32.58795
1205	2:13 PM	1050	526	489	187,306	-117.28059	32.58779
1206	2:16 PM	1050	664	490	203,880	-117.26444	32.58883

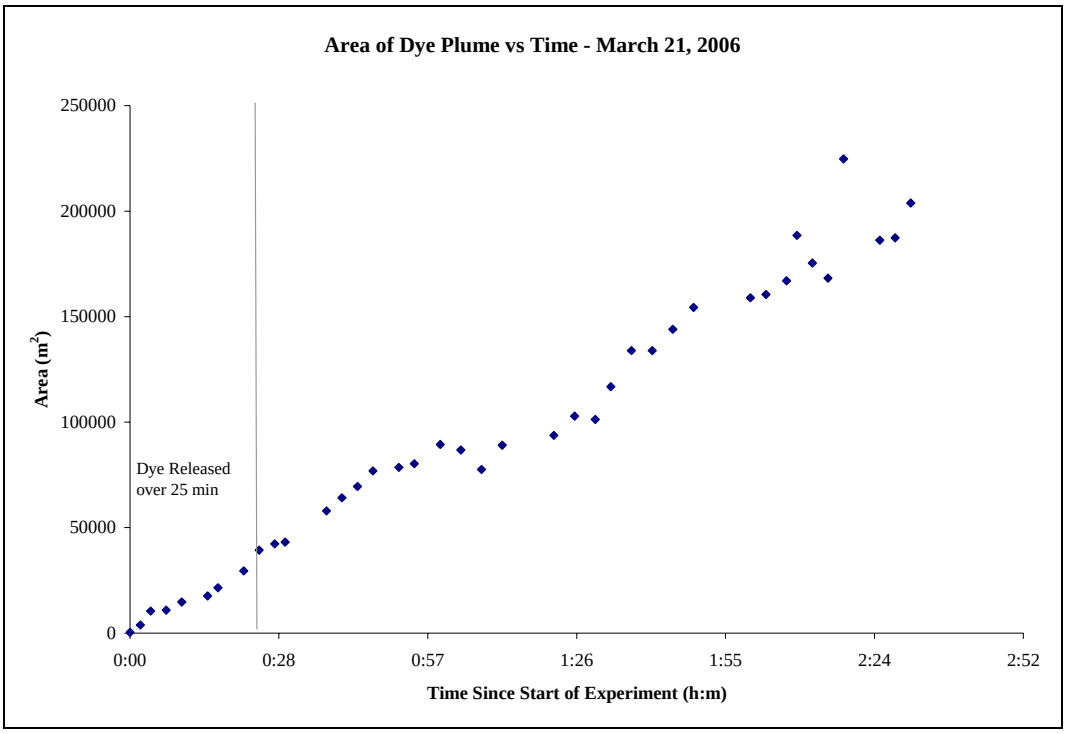

Figure B.3-5. Growth of the area of the plume, as measured from the images.

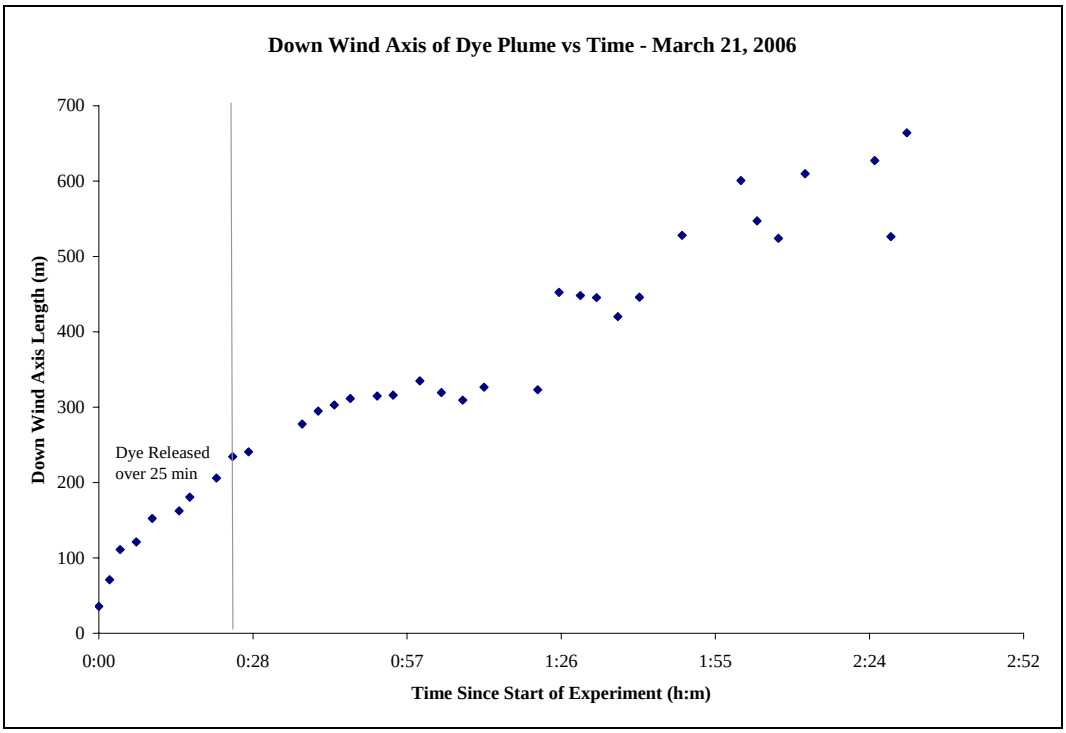

Figure B.3-6. Growth of the down-wind axis of the plume, as measured from the images.

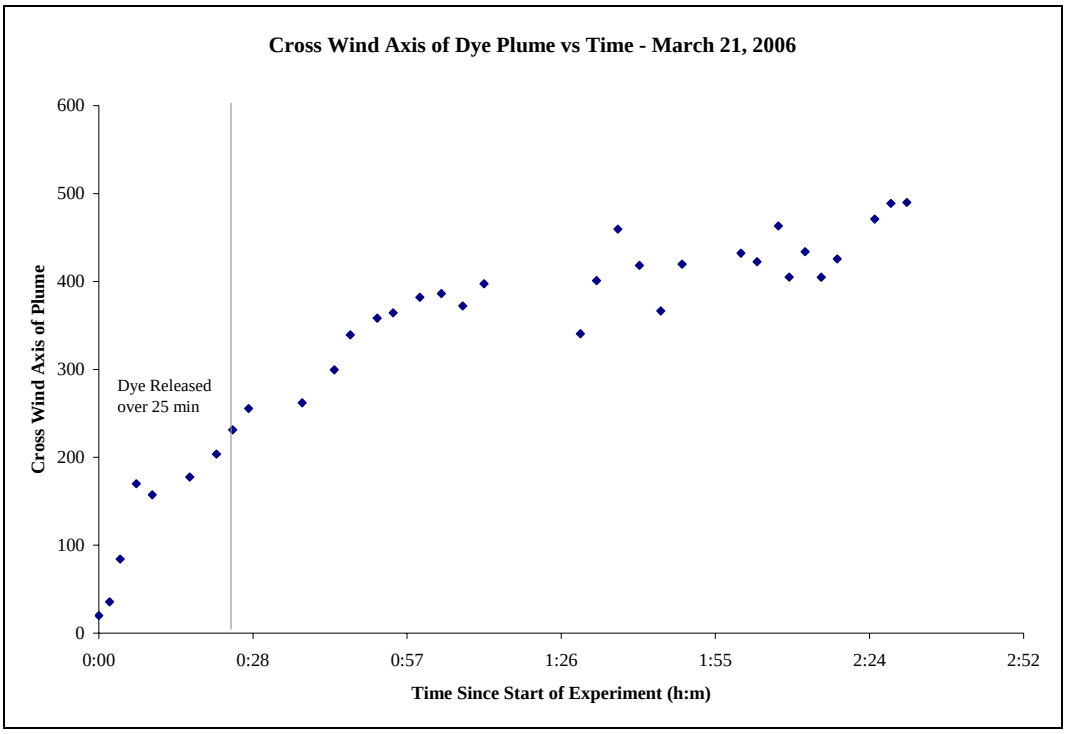

Figure B.3-7. Growth of the cross-wind axis of the plume, as measured from the images.

B.3.3 Langmuir Cell Dimensions Indicated by Dye Images

Measurements of Langmuir cell dimensions for the 21 March experiment are listed in Table B.3-3, and the means are summarized in Table B.3-4. Table B.3-5 lists the mean orientation of Langmuir cells relative to the wind direction as measured at nearby wind stations.

Table B.3-3 Measured dimensions of Langmuir circulation cells for selected images from the 21 March 2006 experiment.

Date	Image name	Time (h:m)	Time after start (h:m)	Sta. LJPC1 Wind dir (degrees)	Sta. LJPC1 Wind speed (knots)	Total width of patch in m (minor axis)	Cell orientation (degrees)	Deviation from wind direction	Major cell spacing (m)	Major cell spacing as % of patch width	Minor cell spacing (m)	Minor cell spacing as % of patch width
3/21/2006	DSC_1134	12:13	0:28	280	11.66	241	323	43	32.4	13.5	9.3	3.9
3/21/2006	DSC_1141	12:29	0:44	280	11.66	305	320	40	32.9	10.8	10.8	3.5
3/21/2006	DSC_1162	1:18	1:33	290	7.78	401	334	44	30.3	7.6	14.1	3.5
3/21/2006	DSC_1184	1:48	2:03	280	9.72	423	308	28	35.7	8.4	9.4	2.2
3/21/2006	DSC_1206	2:16	2:31	280	9.72	490	321	41	37.7	7.7	10.7	2.2
	means			282	10.1	372	321	39	33.8	9.6	10.9	3.1

Table B.3-4. Mean dimensions of Langmuir circulation cells.

Date	Total width of patch in m (minor axis)	Major cell spacing (m)	Major cell spacing as % of patch width	Minor cell spacing (m)	Minor cell spacing as % of patch width
3/21/2006	372	34	10	11	3

Table B.3-5. Orientations of Langmuir circulation cells to the wind direction.

Date	Cell orientation (degrees)	Wind Station	Wind direction (degrees)	Wind speed (knots)	Deviation from wind direction
3/21/2006	321	LJPC1	288	10	34
		46086	302	13	19
		COAMPS	286	14	35

B.4 Results of March 22, 2006 Experiment

B.4.1 Movement and Spreading of Dye

The 22 March 2006 experiment began at 10:00 PST (18:00 UTC) and ended at approximately 14:45 PST (22:45 UTC). The dye plume expanded and moved primarily to east throughout the duration of the experiment. Figure B.4-1 contains a subset of images that show the locations of the dye over time, as interpreted from the aerial photographs. One of the shapes appeared to be displaced far off to the east; however, the other images appear to be accurately located. This displaced shape, which was not used in the analysis, represents one of the images with major georeferencing errors (see section B.1.1 for description of sources of error general to all experiments.) Table B.4-1 lists the file names for the images with major georeferencing errors.

Sources of error specific to date:

- Headings on this date were not recorded digitally. Hand written heading information was tied to the other digital image information based on time. When there was no matching heading record for a given image, the previous heading was used.
- Positional information for the images was transcribed from the image headers in DMS forms, which were then converted to Decimal Degrees. Though the data was checked twice and some transcription errors caught, there is still the potential that transcription errors persisted and affected the locations of the images. The agreement between the dye locations and the drifters, which tracked the dye plume, suggest these errors are small.

Figure B.4-1 contains images of the dye plume over the time of the experiment, overlaid with locations of drifters, as recorded by GPS waypoints. Figure B.4-2 contains the same images of the dye plume over the time, with the centroids of each plotted and labeled with the time of the image. Figures B.4-3 and B.4-4 show example georeferenced images. Figures B.4-3 and B.4-4 also show these images color coded by dye intensity (in arithmetically-scaled bins). Other images are available on the ftp site (see introduction on page 1 of Appendix B).

Table B.4-1. March 22, 2006 images with major georeferencing errors.

Image #	Time (PST)
1227	10:52AM
1248	11:55AM
1250	12:02PM
1292	1:01PM

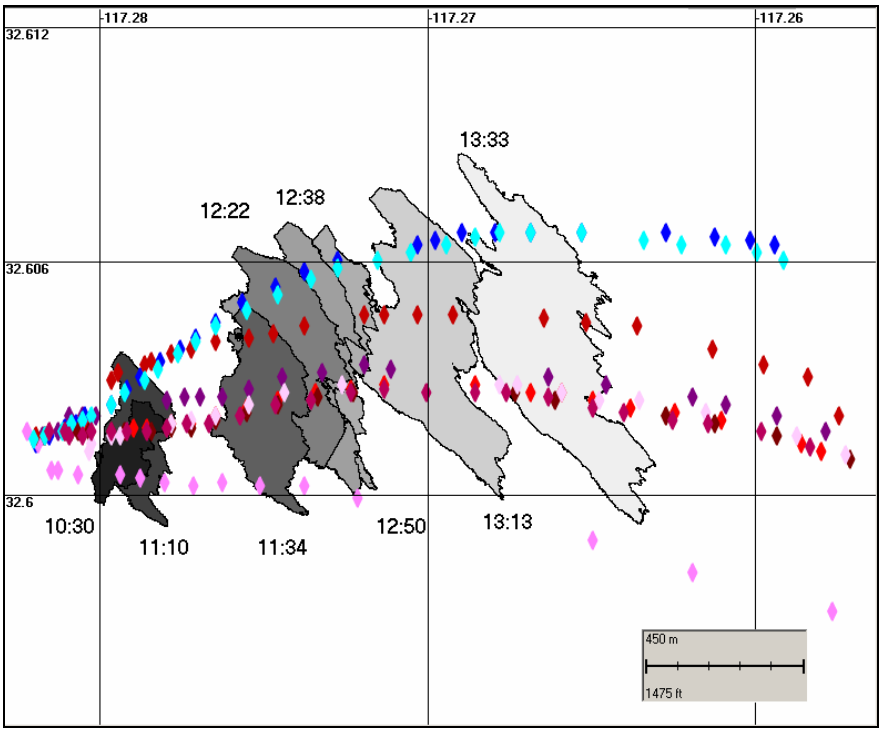

Figure B.4-1. Dye plume dimensions and movements over time, and drifter tracks represented by the diamonds (reds & purples = 1m, blues = 5m deployment depths) for the 22 March 2006 experiment.

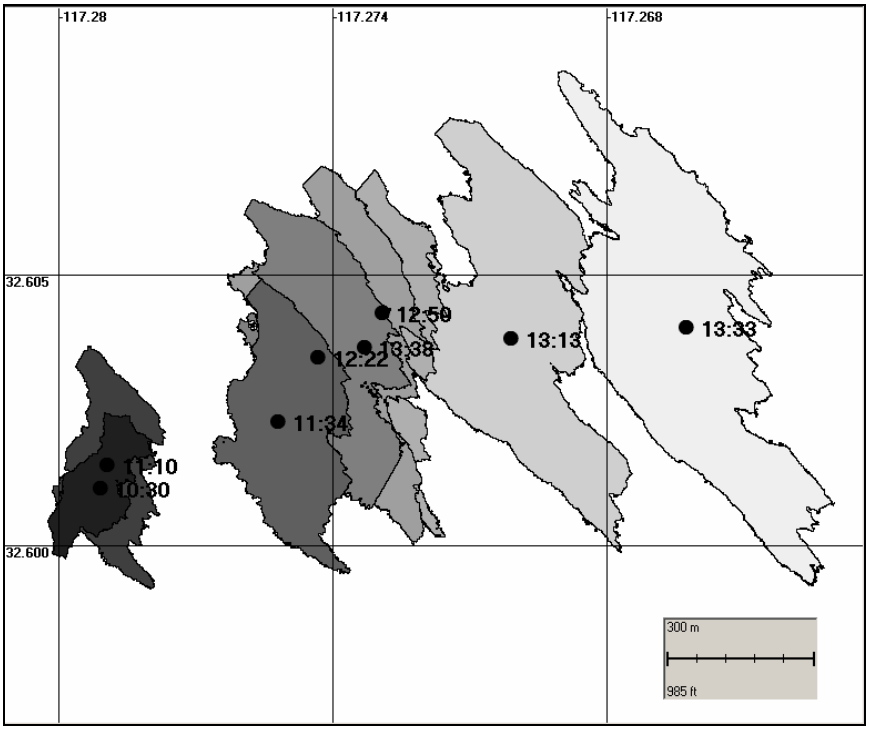

Figure B.4-2. Centroids of selected dye plume images and corresponding times for 22 March 2006 experiment.

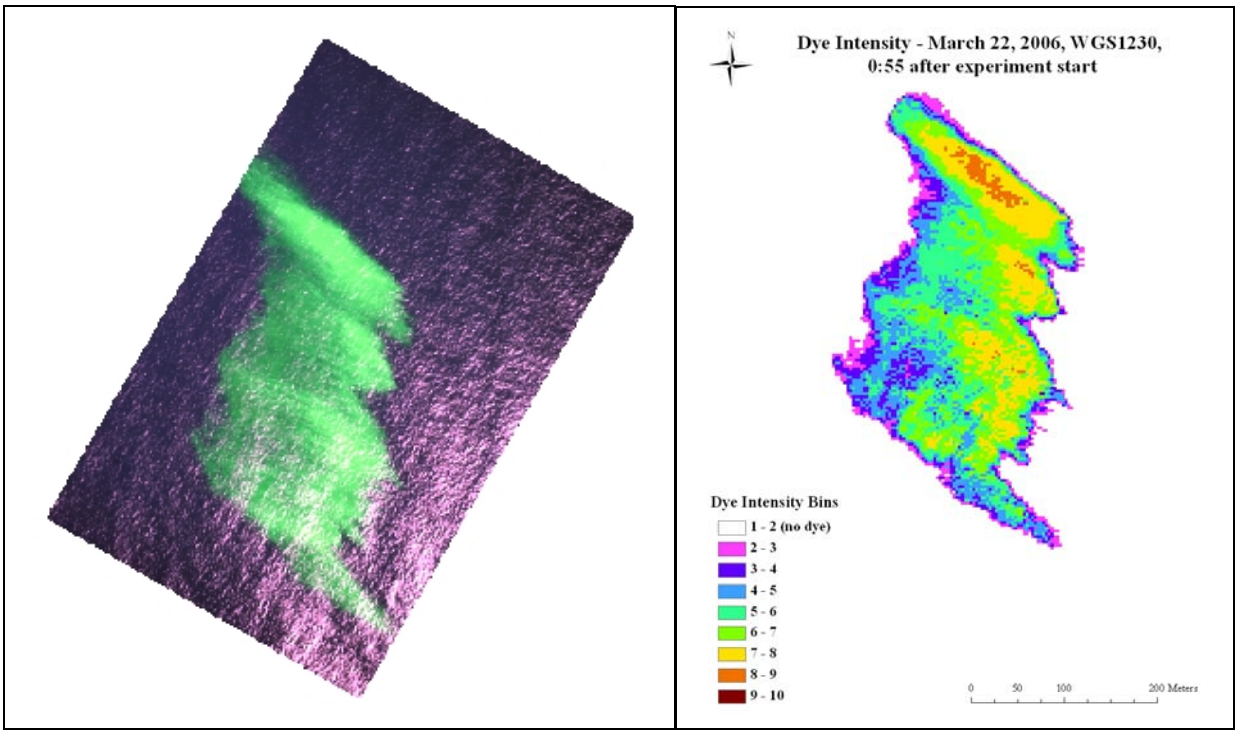

Figure B.4-3. Georectified *.tif and intensity binned (10bin) images of dye plume (image #1230, 11:10 AM on 22 March 2006).

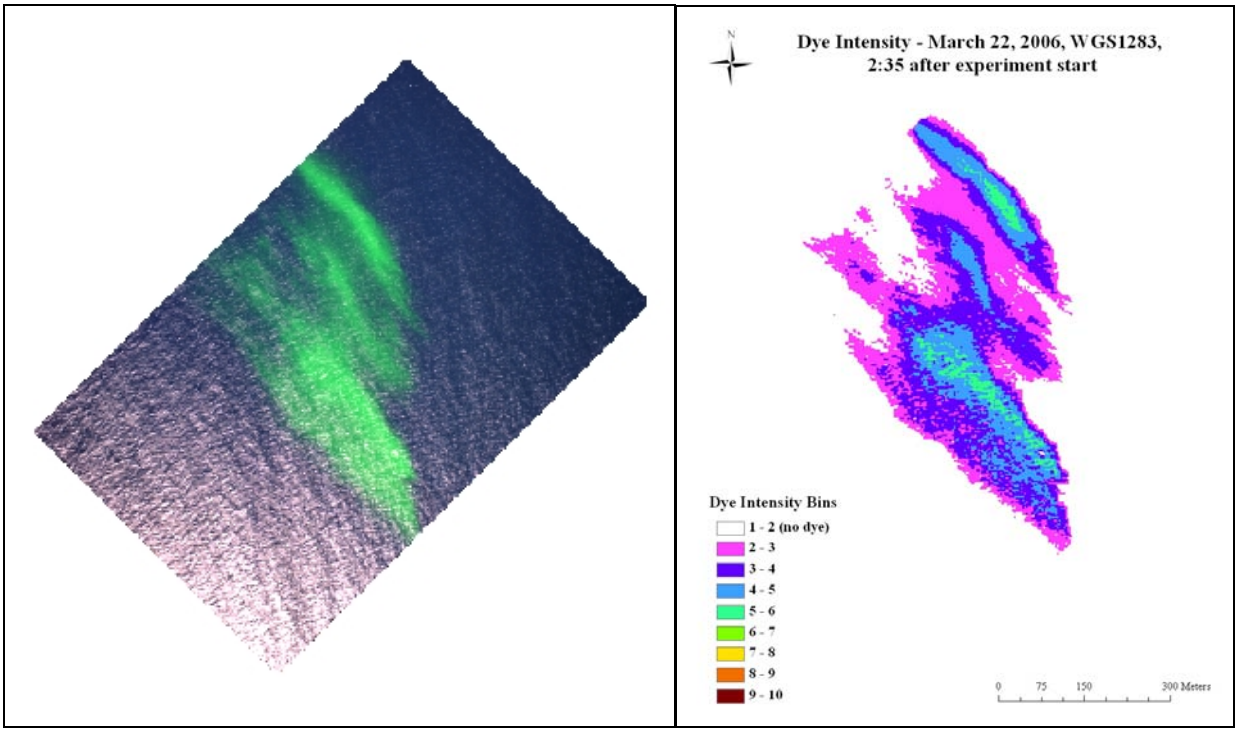

Figure B.4-4. Georectified *.tif and intensity binned (10bin) images of dye plume (image # 1283, 12:50 PM on 22 March 2006).

B.4.2 Dimensions of Dye Over Time

Table B.4-2 lists the images used in the analysis of dye plume dimensions over time. The growth of the area, down-wind axis length and cross-wind axis length over time is plotted in Figures B.4-5 to B.4-7.

Table B.4-2. Data for plume images on 22 March 2006.

Image #	Time (PST)	Altitude (m)	Down-wind axis (m)	Cross-wind axis (m)	Area (m^2)	Centroid (x)	Centroid (y)
1223	10:38 AM	587	141	324	32,135	-117.27719	32.60152
1224	10:43 AM	743	141	349	37,684	-117.27885	32.60093
1225	10:48 AM	732	153	354	39,559	-117.27878	32.60106
1227	10:52 AM	728	161	333	40,864	-117.26012	32.60122
1230	11:10 AM	735	185	343	59,888	-117.27892	32.60147
1237	11:34 AM	1044	253	430	95,083	-117.27511	32.60222
1241	11:40 AM	1034	284	434	106,263	-117.27542	32.60228
1248	11:55 AM	1058	307	352	113,302	-117.33433	32.60274
1250	12:02 PM	1056	331	345	117,339	-117.33632	32.60270
1251	12:02 PM	1057	325	334	121,094	-117.33984	32.60329
1264	12:22 PM	1054	339	332	129,030	-117.27436	32.60355
1266	12:27 PM	1205	389	345	135,826	-117.27242	32.60381
1273	12:38 PM	1193	353	377	127,030	-117.27331	32.60364
1283	12:50 PM	1357	400	360	163,431	-117.27289	32.60424
1292	1:01 PM	1515	410	422	136,768	-117.26563	32.60448
1296.	1:07 PM	1515	448	436	193,500	-117.27041	32.60388
1309	1:22 PM	1516	459	431	251,780	-117.26900	32.60417
1322	1:37 PM	1523	130	361	210,096	-117.26606	32.60382

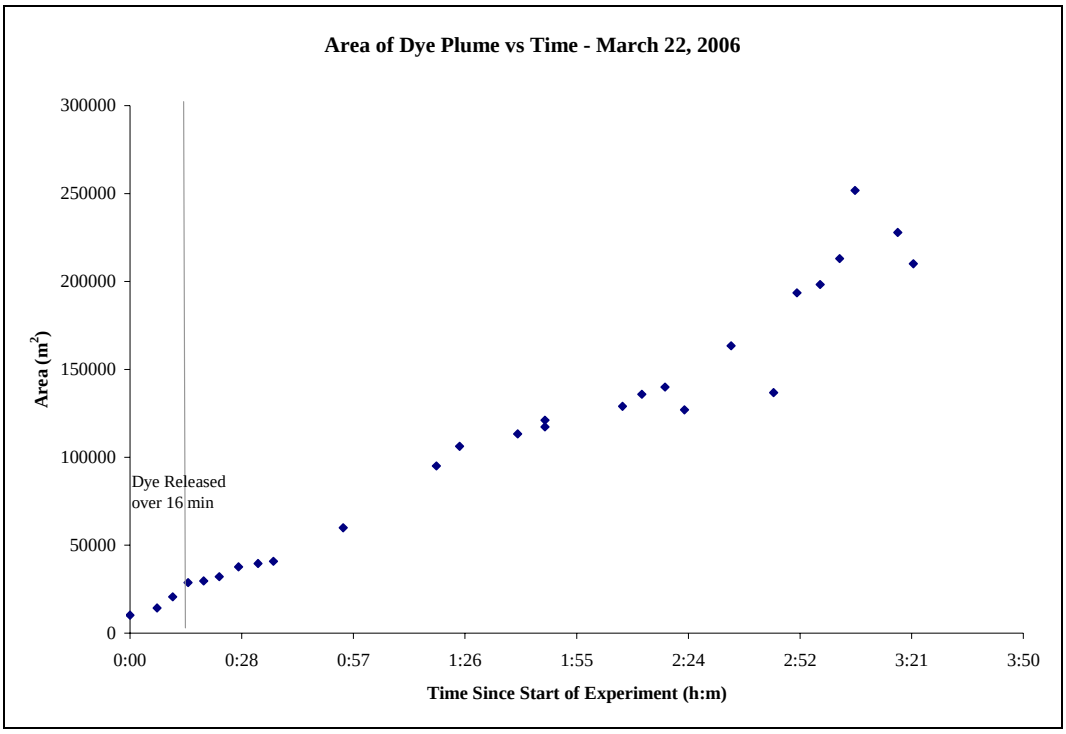

Figure B.4-5. Growth of the area of the plume, as measured from the images.

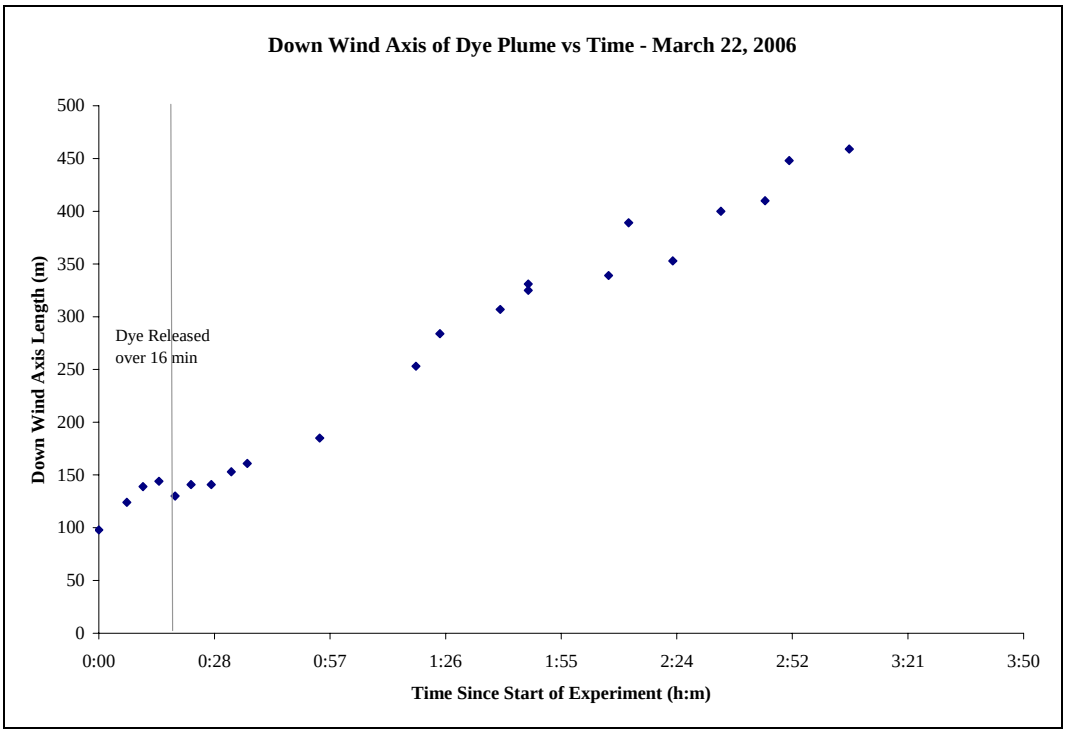

Figure B.4-6. Growth of the down-wind axis of the plume, as measured from the images.

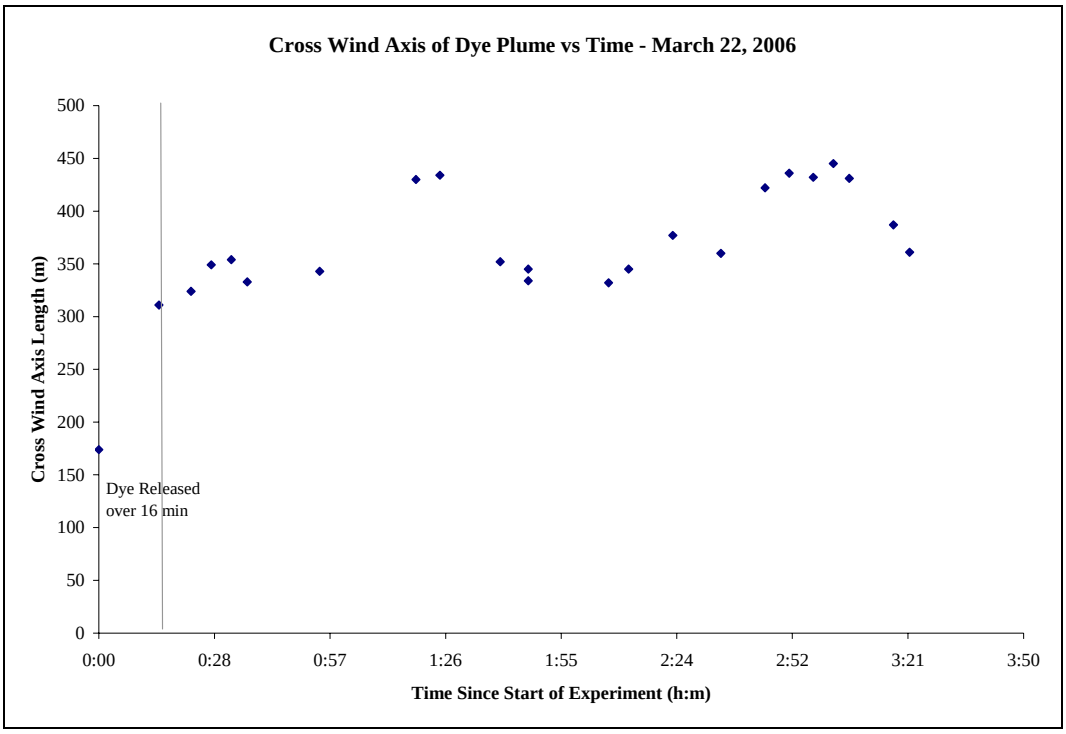

Figure B.4-7. Growth of the cross-wind axis of the plume, as measured from the images.

B.4.3 Langmuir Cell Dimensions Indicated by Dye Images

Measurements of Langmuir cell dimensions for the 22 March experiment are listed in Table B.4-3 and the means are summarized in Table B.4-4. Table B.4-5 lists the mean orientation of Langmuir cells relative to the wind direction as measured at nearby wind stations.

Table B.4-3 Measured dimensions of Langmuir circulation cells for selected images from the 22 March 2006 experiment.

Date	Image name	Time (h:m)	Time after start (h:m)	Sta. LJPC1 Wind dir (degrees)	Sta. LJPC1 Wind speed (knots)	Total width of patch in m (minor axis)	Cell orientation (degrees)	Deviation from wind direction	Major cell spacing (m)	Major cell spacing as % of patch width	Minor cell spacing (m)	Minor cell spacing as % of patch width
3/22/2006	DSC_1224	10:43	0:28	310	5.83	157	314	4	23.7	15.1	4.9	3.1
3/22/2006	DSC_1227	10:52	0:37	310	5.83	175	300	-10	35.3	20.2	5.0	2.8
3/22/2006	DSC_1241	11:40	1:25	320	7.78	322	307	-13	106.0	32.9	9.1	2.8
3/22/2006	DSC_1251	12:02	1:47	320	7.78	332	314	-6	92.0	27.7	12.8	3.8
3/22/2006	DSC_1273	12:38	2:23	320	9.72	353	327	7	97.5	27.6	15.7	4.5
	means			316	7.4	268	312	-4	70.9	24.7	9.5	3.4

Table B.4-4. Mean dimensions of Langmuir circulation cells.

Date	Total width of patch in m (minor axis)	Major cell spacing (m)	Major cell spacing as % of patch width	Minor cell spacing (m)	Minor cell spacing as % of patch width
3/22/2006	268	71	25	10	3

Table B.4-5. Orientations of Langmuir circulation cells to the wind direction.

Date	Cell orientation (degrees)	Wind Station	Wind direction (degrees)	Wind speed (knots)	Deviation from wind direction
3/22/2006	312	LJPC1	318	7	-5
		4608	347	10	-34
		COAMPS	302	9	10

B.5 Results of June 21, 2006 Experiment

B.5.1 Movement and Spreading of Dye

The 21 June 2006 experiment began at 12:11 PDT (19:11 UTC) and ended at approximately 16:00 PDT (23:00 UTC). Figure B.5-1 contains a subset of images that show the locations of the dye over time, as interpreted from the aerial photographs. While there were still sources of georeferencing errors for images from this experiment, they were not as great as previous dates (see section B.1.1 for description of sources of error general to all experiments).

Sources of error specific to date:

- Plane heading information was not recorded for this date. Therefore, heading information was "calculated" using the aircraft positions at the time of a given image and the time immediately before the image. The orientation of the line connecting the two positions was used as the heading. This resulted in approximate and inaccurate headings and could not be applied to all of the images (i.e., those at the beginning of a pass – no prior position).

Figure B.5-1 contains images of the dye plume over the time of the experiment, overlaid with locations of drifters, as recorded by GPS waypoints. Figure B.5-2 contains the same images of the dye plume over the time, with the centroids of each plotted and labeled with the time of the image. Figures B.5-3 and B.5-4 show example georeferenced images. Figures B.5-3 and B.5-4 also show these images color coded by dye intensity (in arithmetically-scaled bins). Other images are available on the ftp site (see introduction on page 1 of Appendix B).

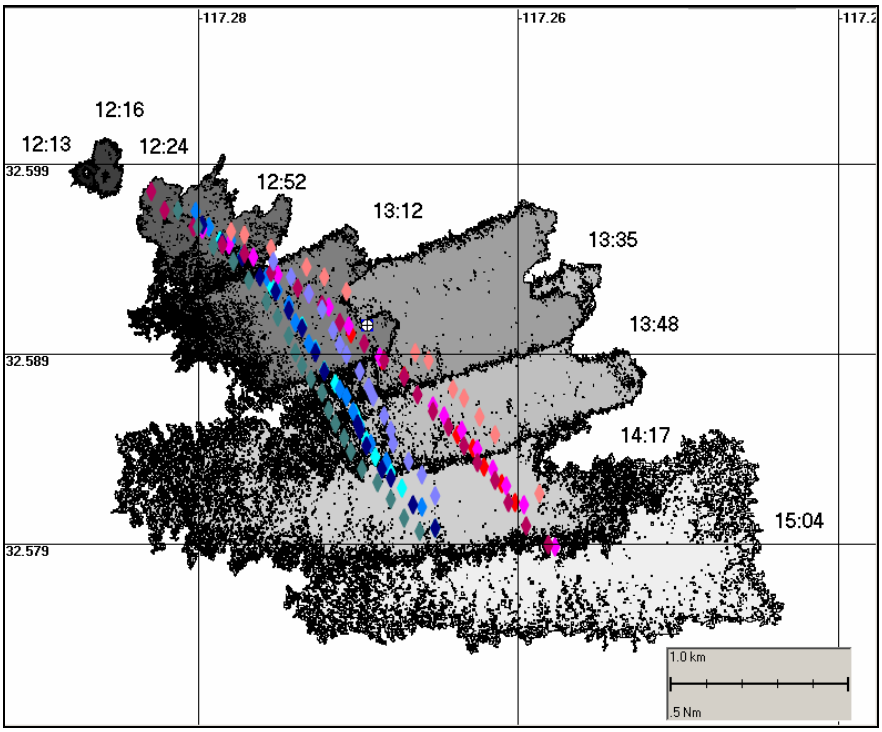

Figure B.5-1. Dye plume dimensions and movements over time, and drifter tracks represented by the diamonds (reds & purples = 2m, blues = 4m deployment depths) for the 21 June 2006 experiment.

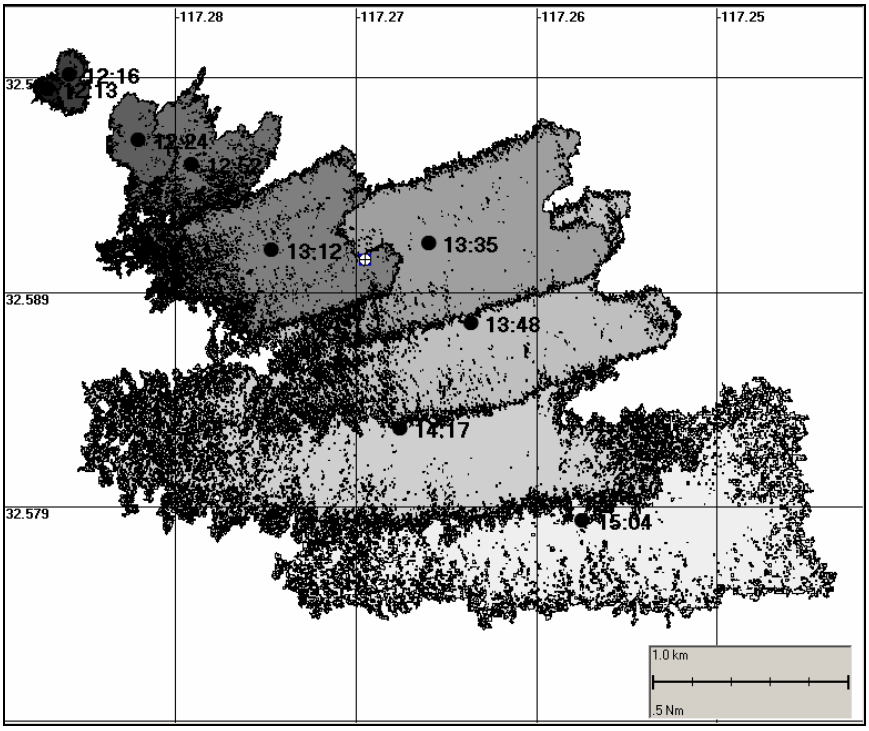

Figure B.5-2. Centroids of selected dye plume images and corresponding times on 21 June 2006.

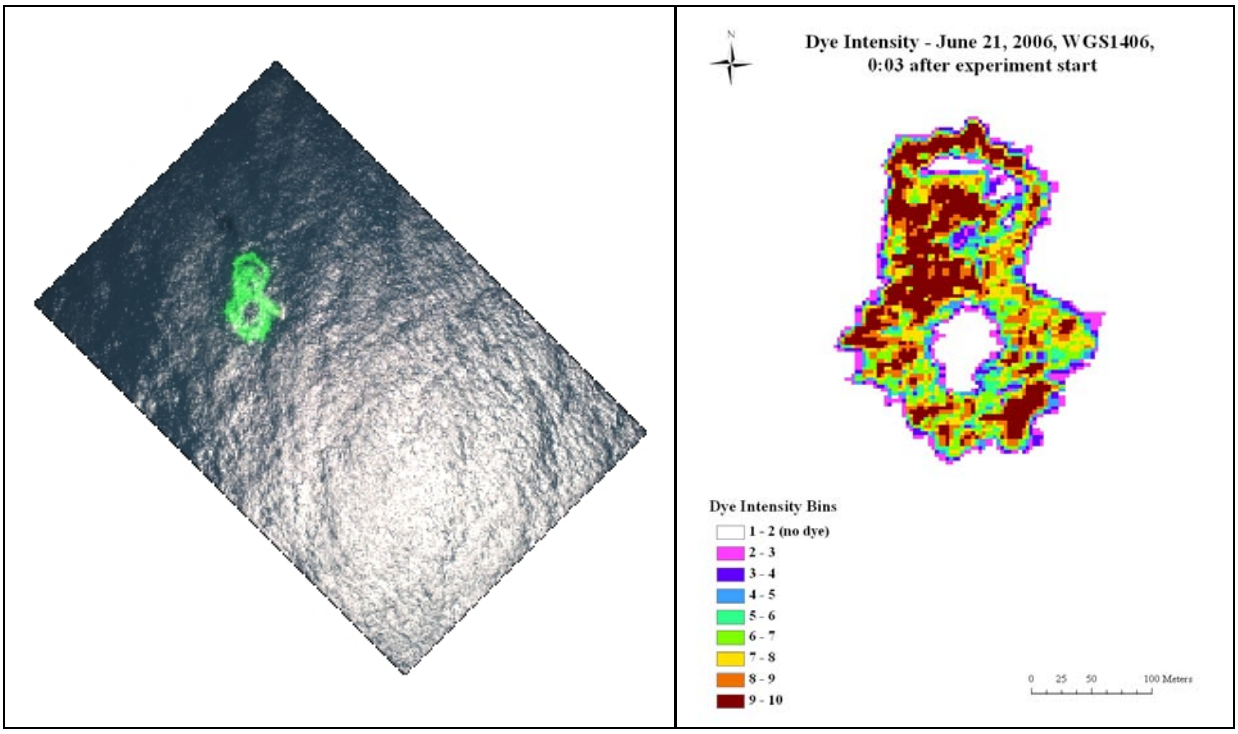

Figure B.5-3. Georectified *.tif and intensity binned (10bin) images of dye plume (image #1406, 12:16 PM on 21 June 2006).

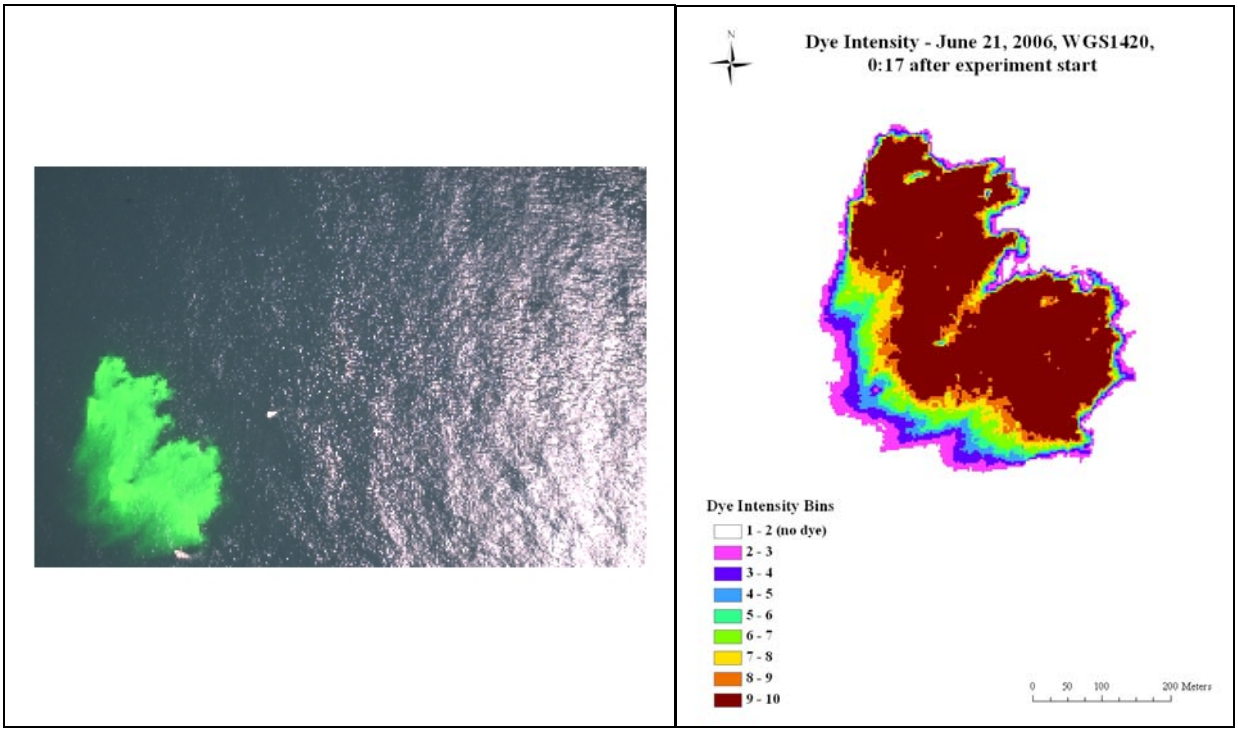

Figure B.5-4. Georectified *.tif and intensity binned (10bin) images of dye plume (image #1420, 12:30 PM on 21 June 2006).

B.5.2 Dimensions of Dye Over Time

Table B.5-1 lists the images used in the analysis of dye plume dimensions over time. The growth of the area, down-wind axis length and cross-wind axis length over time is plotted in Figures B.5-5 to B.5-7.

Table B.5-1. Data for plume images on 21 June 2006.

Image #	Time (PDT)	Down-wind axis (m)	Cross-wind axis (m)	Area (m^2)	Centroid (x)	Centroid (y)
1424	12:33 PM	454	603	149,746	-117.28198	32.59585
1427	12:36 PM	479	650	160,035	-117.28198	32.59516
1430	12:39 PM	665	666	280,636	-117.28299	32.59712
1439	12:46 PM	1012	672	426,010	-117.28347	32.59665
1441	12:49 PM	962	685	387,659	-117.27684	32.59460
1443	12:52 PM	1017	644	340,175	-117.27899	32.59593
1446	12:56 PM	1179	684	417,490	-117.27788	32.59562
1449	12:59 PM	1017	711	429,210	-117.27400	32.59570
1452	1:03 PM	1224	750	586,634	-117.27709	32.59110
1455	1:07 PM	1165	760	502,993	-117.27320	32.59463
1459	1:12 PM	1489	827	700,621	-117.27455	32.59194
1463	1:17 PM	1689	807	782,636	-117.27389	32.59292
1472	1:35 PM	2067	878	1,207,817	-117.26590	32.59222
1476	1:39 PM	1978	921	1,108,044	-117.27062	32.58619
1483	1:43 PM	2208	910	1,282,807	-117.26520	32.59173
1487	1:47 PM	2445	966	1,427,575	-117.26568	32.59192
1490	1:48 PM	2403	936	1,358,815	-117.26346	32.58843
1493	1:54 PM	2890	988	1,704,710	-117.26366	32.59124
1498	1:59 PM	2790	1016	1,786,462	-117.26142	32.58832
1501	2:04 PM	2721	1093	1,554,109	-117.26730	32.59061
1504	2:05 PM	2776	1038	1,561,411	-117.26668	32.58650
1507	2:11 PM	3208	1099	1,979,506	-117.26162	32.58566
1512	2:17 PM	3237	1241	2,034,942	-117.26754	32.58346
1521	2:23 PM	3367	1284	2,374,196	-117.25957	32.57682
1528	2:27 PM	3744	1202	2,346,993	-117.26005	32.58197
1535	2:39 PM	3405	1260	2,430,188	-117.26019	32.57847
1544	2:50 PM	3452	1207	2,264,150	-117.25896	32.57524
1555	2:54 PM	3474	1280	2,233,430	-117.26179	32.58168

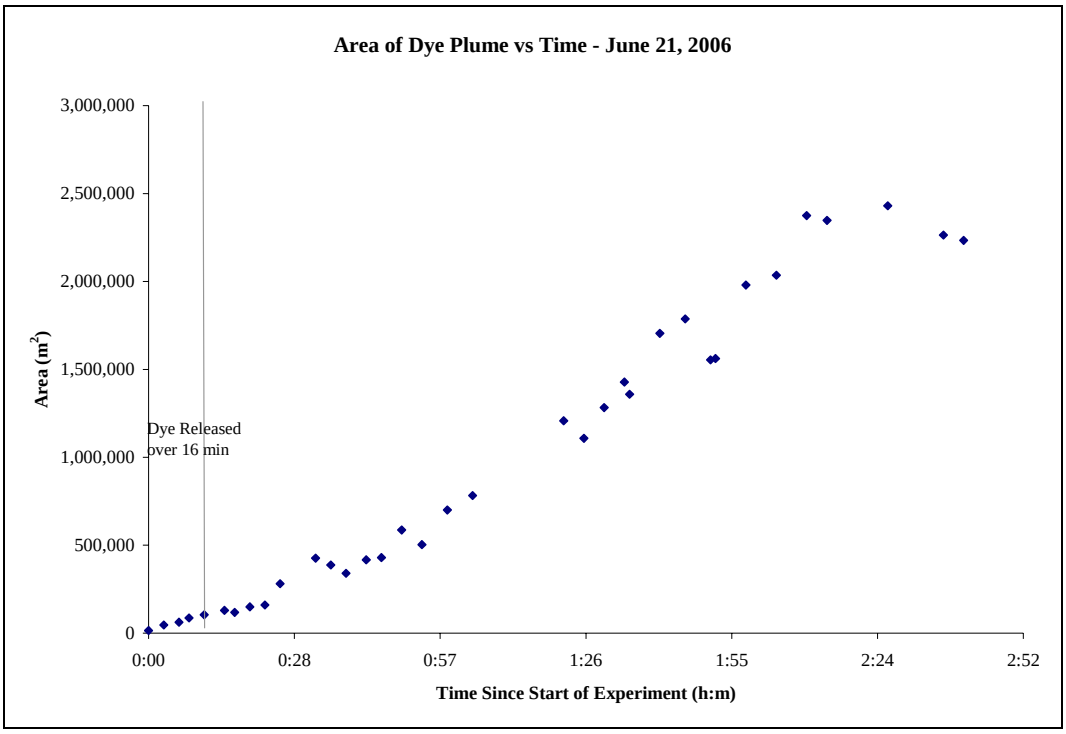

Figure B.5-5. Growth of the area of the plume, as measured from the images.

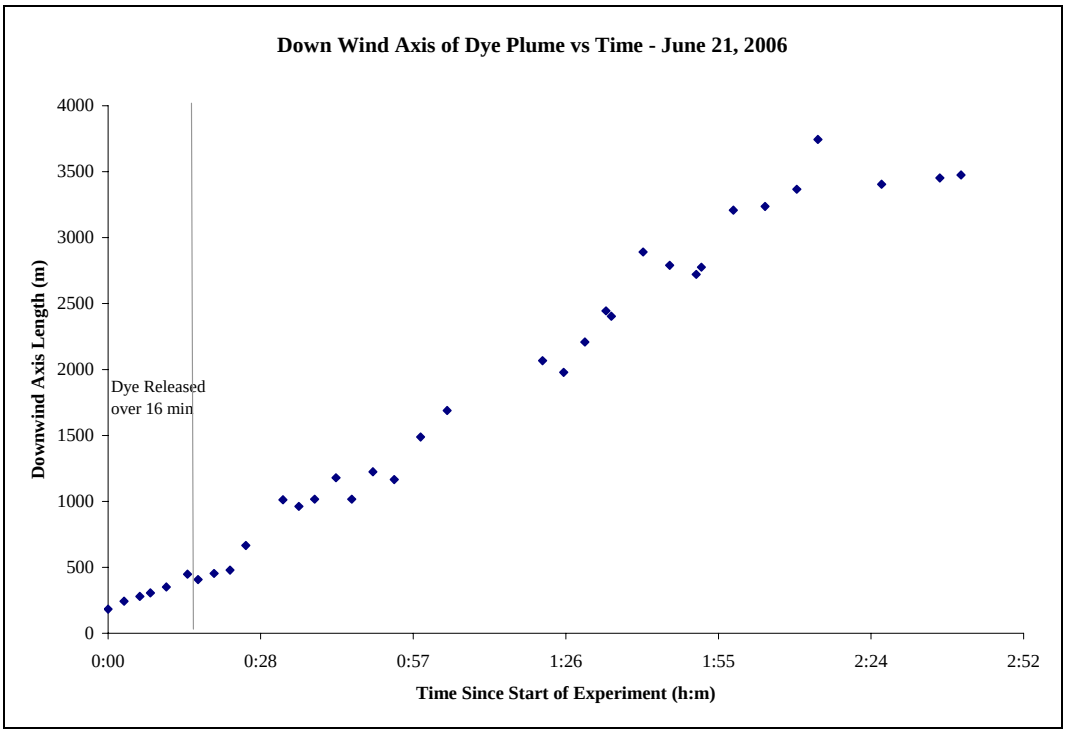

Figure B.5-6. Growth of the down-wind axis of the plume, as measured from the images.

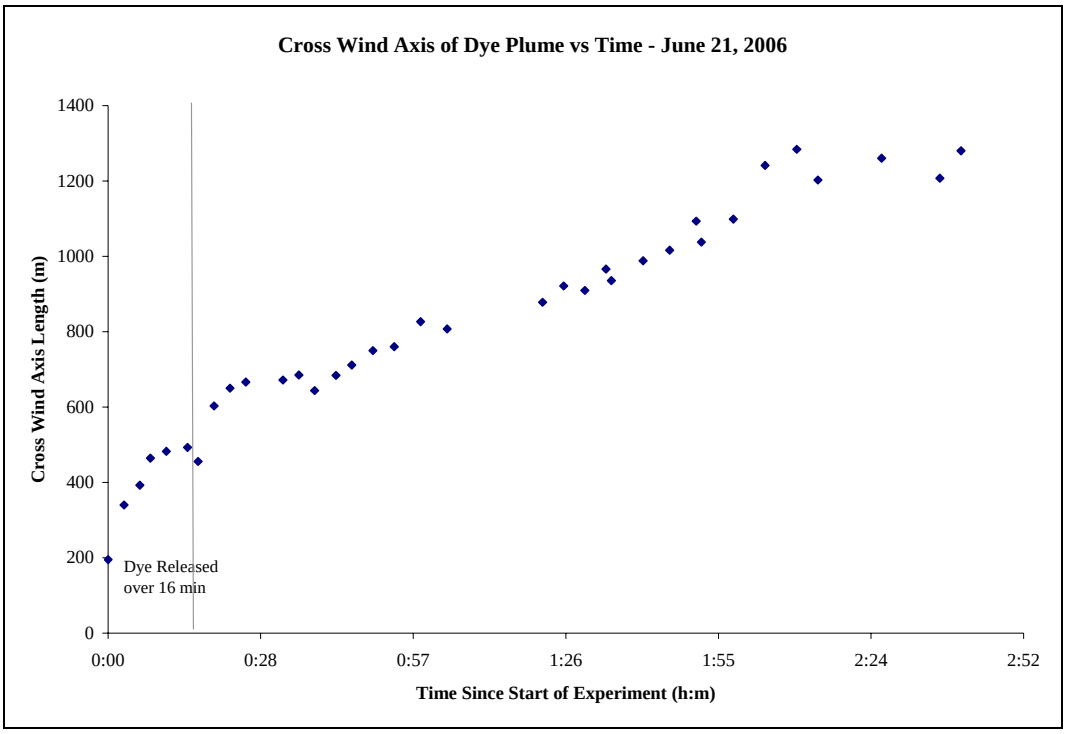

Figure B.5-7. Growth of the cross-wind axis of the plume, as measured from the images.

B.6 Results of June 22, 2006 Experiment

B.6.1 Movement and Spreading of Dye

The 22 June 2006 experiment began at 14:49 PDT (21:49 UTC) and ended at approximately 17:50 PDT (00:50 UTC, 23 June). The dye plume expanded and moved primarily to the east throughout the duration of the experiment. Figure B.6-1 contains a subset of images that show the locations of the dye over time, as interpreted from the aerial photographs. Several of the photographs taken on this date did not capture the full extent of the dye plume and were cut off. Composite images were made by piecing together various photographs to capture the full plume dimension at approximate times. Table B.6-1 lists the file names for the images that were composited in this experiment to create shape files of the entire plume at those times. While there were still sources of georeferencing errors for images from this experiment, they were not as great as previous dates (see section B.1.1 for description of sources of error general to all experiments.)

Figure B.6-1 contains images of the dye plume over the time of the experiment, overlaid with locations of drifters, as recorded by GPS waypoints. Figure B.6-2 contains the same images of the dye plume over the time, with the centroids of each plotted and labeled with the time of the image. Figures B.6-3 and B.6-4 show example georeferenced images. Figures B.6-3 and B.6-4 also show these images color coded by dye intensity (in arithmetically-scaled bins). Other images are available on the ftp site (see introduction on page 1 of Appendix B).

Table B.6.1. List of composite images for 22 June 2006 experiment.

Image #	Time (PDT)
1657_58	3:06 PM
1661_62_63	3:10 PM
1667_68	3:15 PM
1678_80	3:25 PM
1685_87	3:29 PM
1696_98_99	3:35 PM
1713_17_18	3:48 PM
1723_27_28	3:52 PM
1758_63_67	4:05 PM
1769_74_76	4:10 PM
1833_37_38	4:42 PM
1848_49_50	4:47 PM

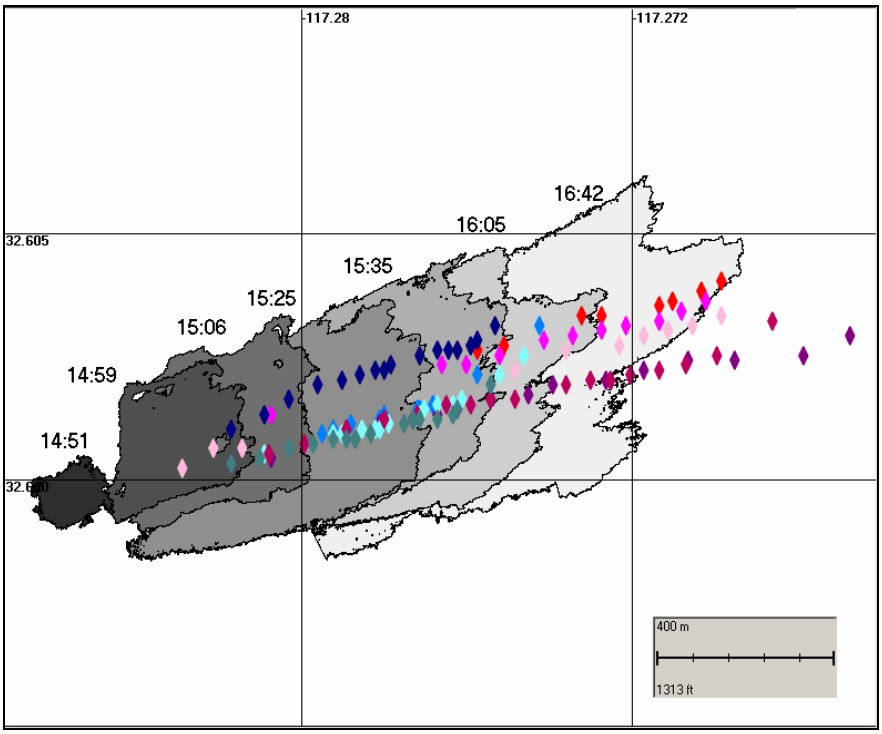

Figure B.6-1. Dye plume dimensions and movements over time and drifter tracks represented by the diamonds (reds & purples = 2m and blues = 4m deployment depths) for the 22 June 2006 experiment.

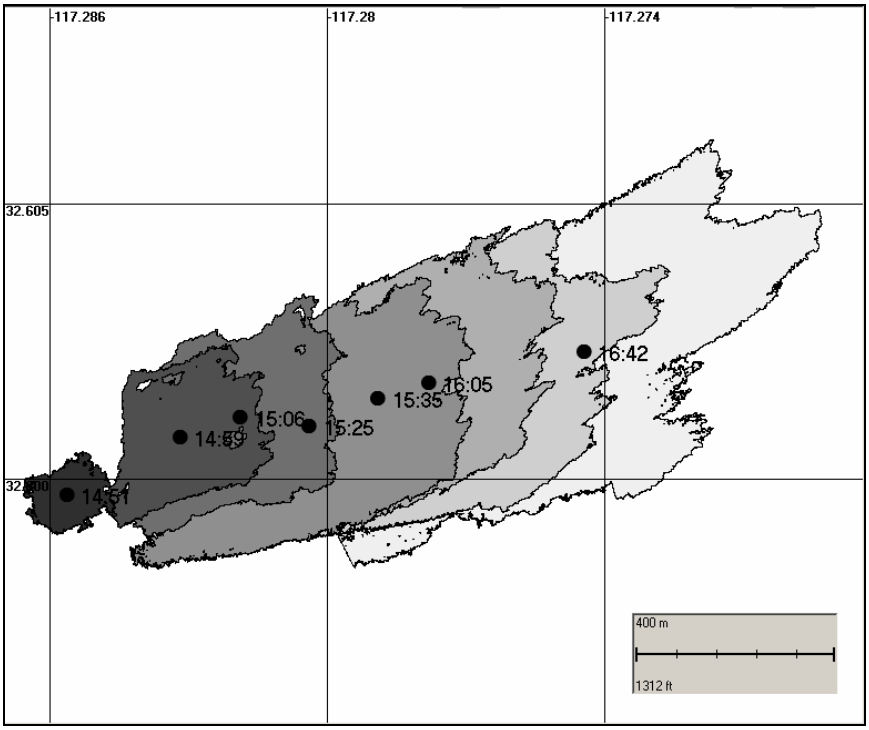

Figure B.6-2. Centroids of selected dye plume images and corresponding times on 22 June 2006.

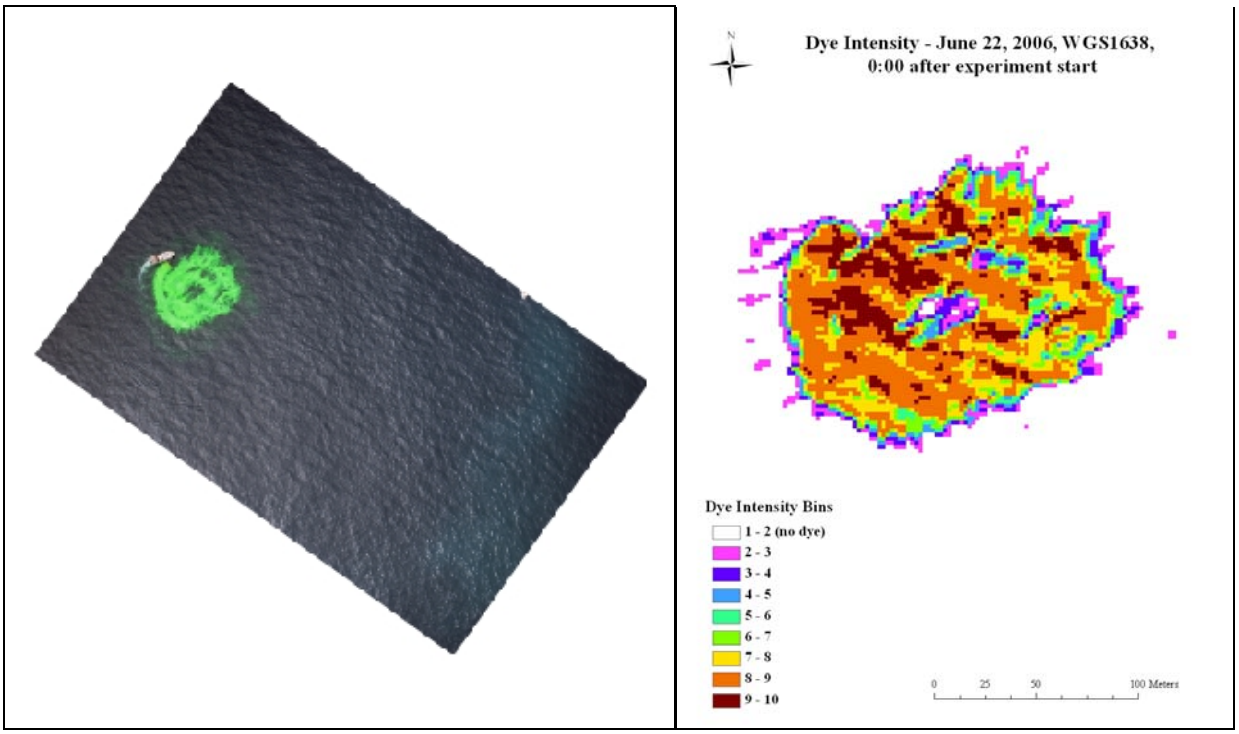

Figure B.6-3. Georectified *.tif and intensity binned (10bin) images of dye plume (image #1638, 2:51PM on 22 June 2006).

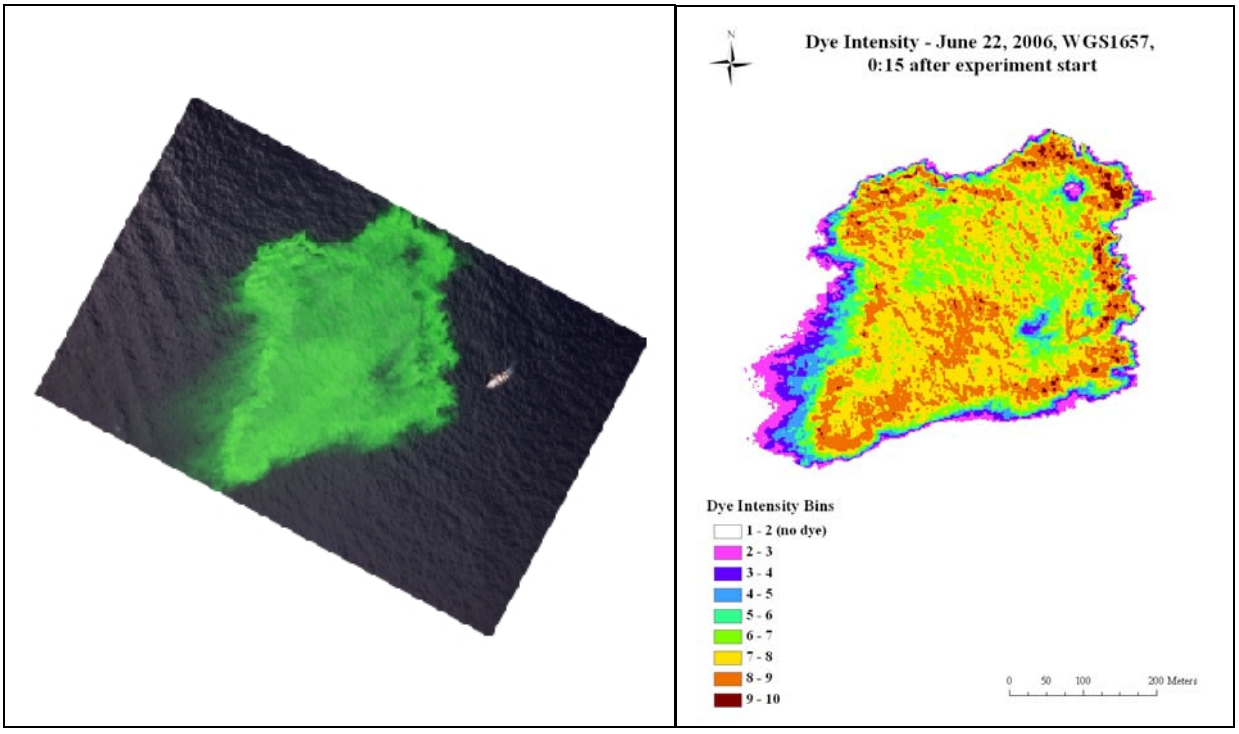

Figure B.6-4. Georectified *.tif and intensity binned (10bin) images of dye plume (image #1657, 3:07PM on 22 June 2006).

B.6.2 Dimensions of Dye Over Time

Table B.6-2 lists the images used in the analysis of dye plume dimensions over time. The growth of the area, down-wind axis length and cross-wind axis length over time is plotted in Figures B.6-5 to B.6-7.

Table B.6-2. Plume data for each image of the 22 June 2006 experiment.

Image #	Time (PDT)	Down-wind axis (m)	Cross-wind axis (m)	Area (m^2)	Centroid (x)	Centroid (y)
1661_62_63	3:10 PM	572	407	153,996	-117.28142	32.60011
1667_68	3:15 PM	594	416	159,660	-117.27975	32.60003
1678_80	3:25 PM	787	451	227,023	-117.28042	32.60086
1685_87	3:29 PM	796	441	244,188	-117.27977	32.60083
1696_98_99	3:35 PM	921	455	258,692	-117.27880	32.60147
1713_17_18	3:48 PM	1005	479	310,839	-117.28011	32.60101
1723_27_28	3:52 PM	1191	503	358,987	-117.27866	32.60058
1848_49_50	4:47 PM	572	560	346,844	-117.27439	32.60129

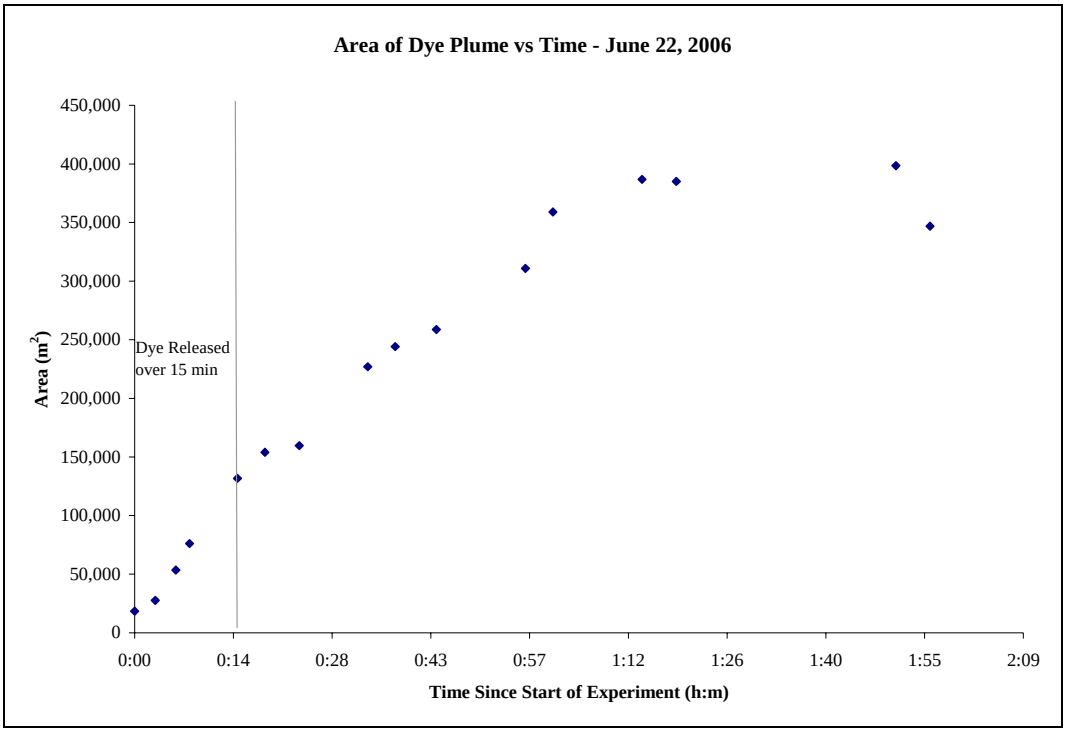

Figure B.6-5. Growth of the area of the plume, as measured from the images.

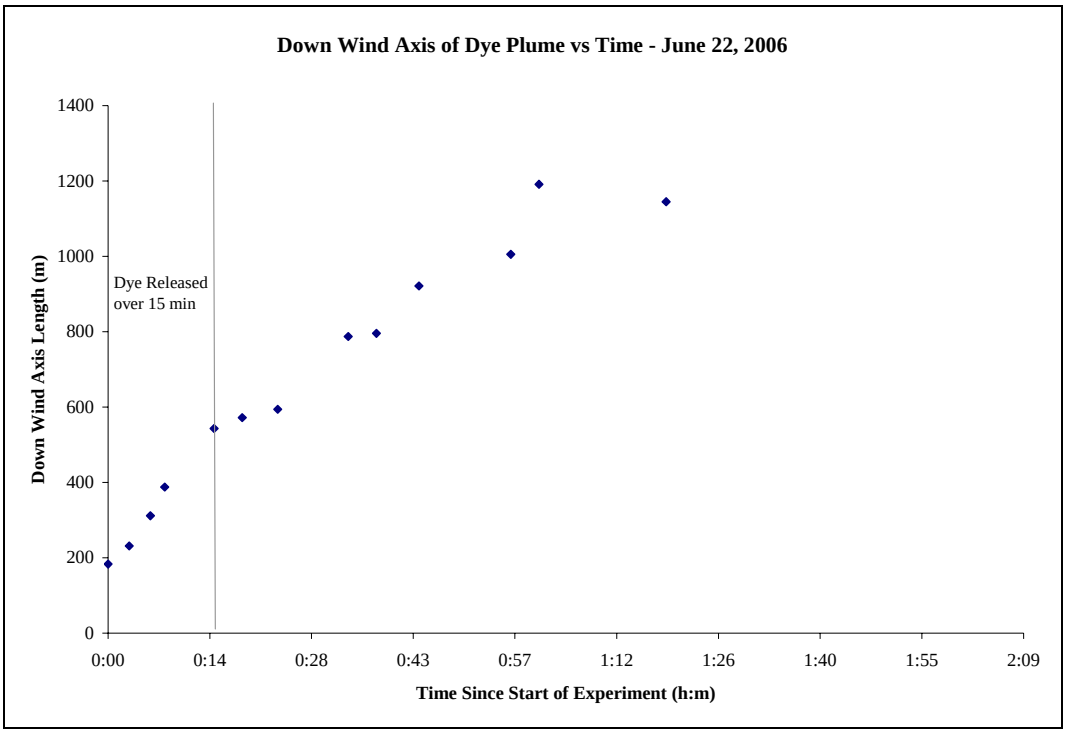

Figure B.6-6. Growth of the down-wind axis of the plume, as measured from the images.

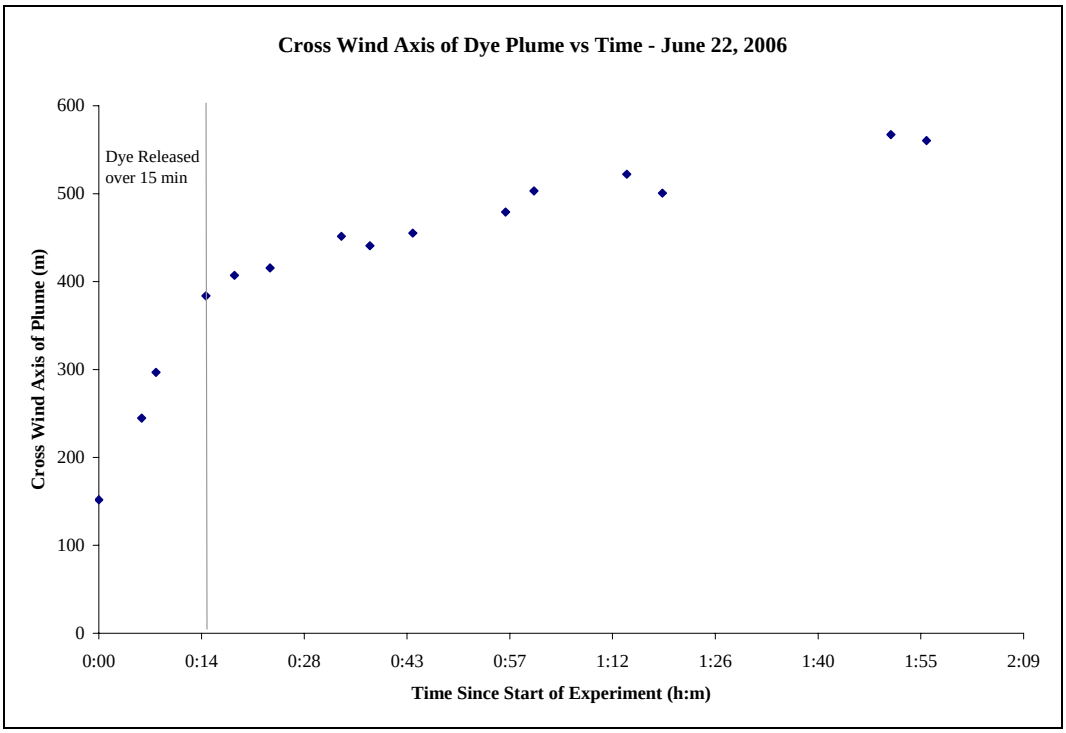

Figure B.6-7. Growth of the cross-wind axis of the plume, as measured from the images.

B.7 Results of November 1, 2006 Experiment

B.7.1 Movement and Spreading of Dye

The 1 November 2006 experiment began at 11:50 PST (19:50 UTC) and ended at approximately 15:30 PST (23:30 UTC). The dye plume expanded and moved primarily to the south and then southeast throughout the duration of the experiment. Figure B.7-1 contains a subset of images that show the locations of the dye over time, as interpreted from the aerial photographs. Some of the photographs taken on this date did not capture the full extent of the dye plume and were cut off. Composite images were made by piecing together various photographs to capture the full plume dimension at approximate times. Table B.7-1 lists the file names for the images that were composited in this experiment to create shape files of the entire plume at those times. While there were still sources of georeferencing errors for images from this experiment, they were not as great as previous dates (see section B.1.1 for description of sources of error general to all experiments.)

Figure B.7-1 contains images of the dye plume over the time of the experiment, overlaid with locations of drifters, as recorded by GPS waypoints. Figure B.7-2 contains the same images of the dye plume over the time, with the centroids of each plotted and labeled with the time of the image. Figures B.7-3 and B.7-4 show example georeferenced images. Figures B.7-3 and B.7-4 also show these images color coded by dye intensity (in arithmetically-scaled bins). Other images are available on the ftp site (see introduction on page 1 of Appendix B).

Table B.7-1. List of composite images for 1 November 2006 experiment.

Image #	Time (PST)
0465_0468	12:53 PM
0516_0517	1:32 PM
0555_0556	2:02 PM
0626_0627	2:50 PM
0645_0646	3:04 PM
0660_0661	3:12 PM

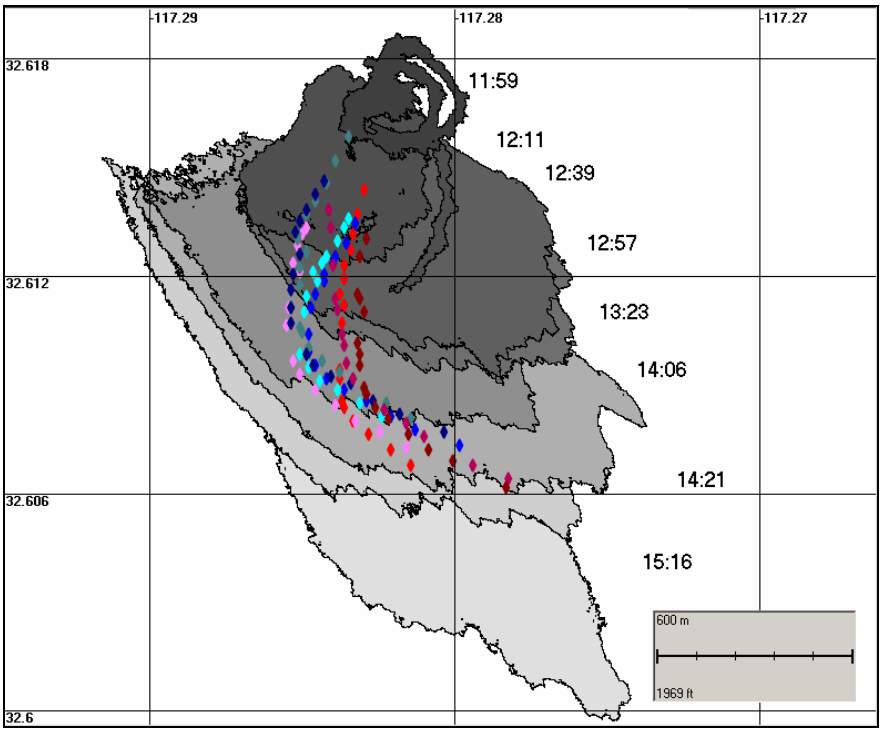

Figure B.7-1. Dye plume dimensions and movements over time, and drifter tracks represented by the diamonds (reds & purples = 2m, blues = 4m deployment depths) for the 1 November 2006 experiment.

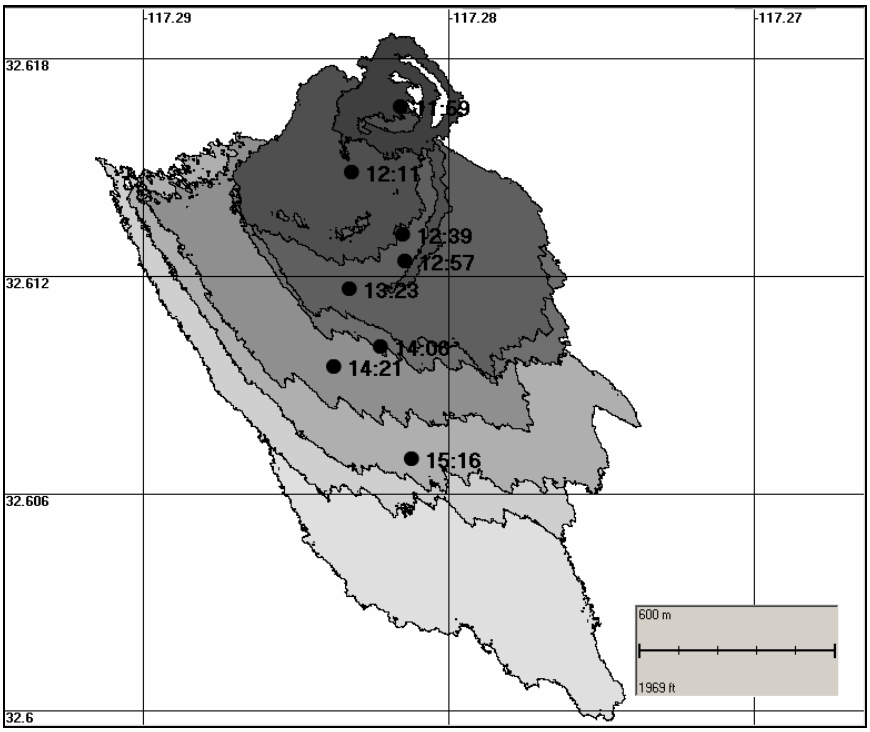

Figure B.7-2. Centroids of selected dye plume images and corresponding times on 1 November 2006).

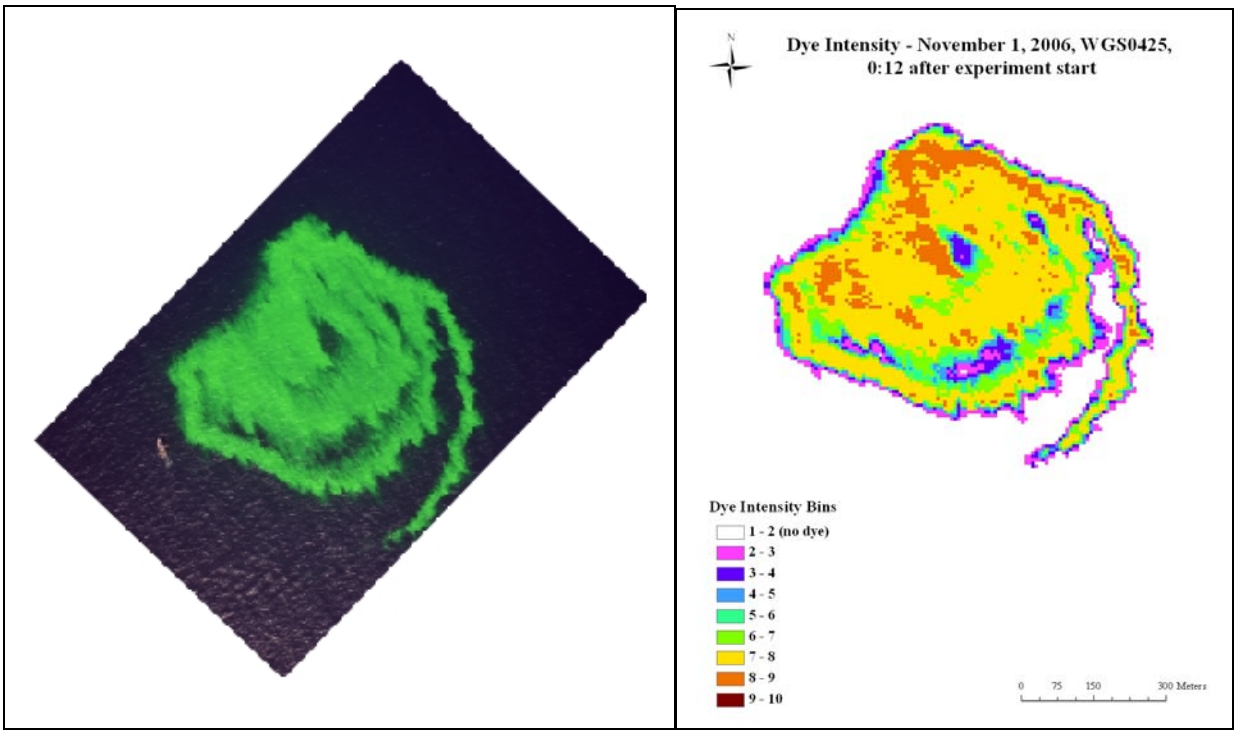

Figure B.7-3. Georectified *.tif images of dye plume (image #0425, 12:11 PM on 1 November 2006).

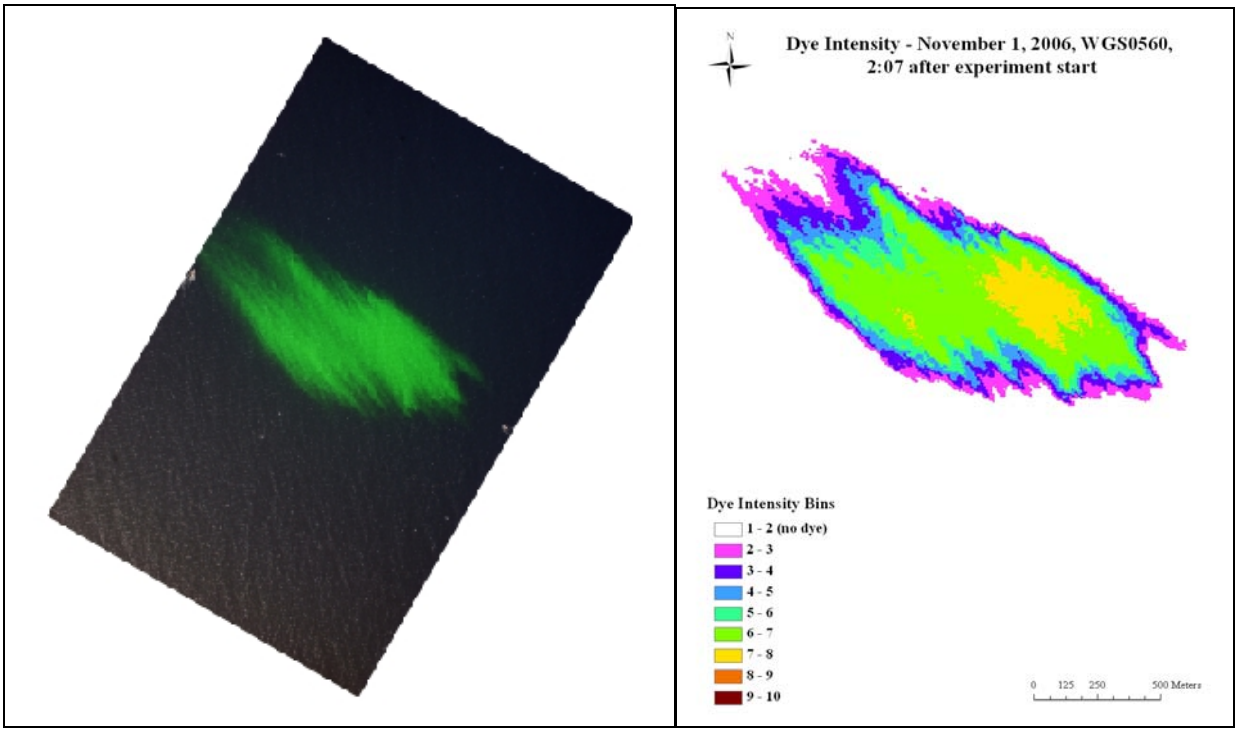

Figure B.7-4. Georectified *.tif images of dye plume (image #0560, 2:06 PM on 1 November 2006).

B.7.2 Dimensions of Dye Over Time

Table B.7-2 lists the images used in the analysis of dye plume dimensions over time. The growth of the area, down-wind axis length and cross-wind axis length over time is plotted in Figures B.7-5 to B.7-7.

Table B.7-2. Data for all plume images of the 1 November 2006 experiment.

Image #	Time (PST)	Down-wind axis (m)	Cross-wind axis (m)	Area (m^2)	Centroid (x)	Centroid (y)
0432	12:20 PM	796	601	356,085	-117.28161	32.61320
0436	12:25 PM	850	629	403,342	-117.28072	32.61276
0439	12:30 PM	886	649	432,295	-117.28002	32.61366
0445	12:35 PM	975	660	471,893	-117.28149	32.61464
0450	12:39 PM	1052	661	500,339	-117.28146	32.61310
0453	12:44 PM	1071	655	496,476	-117.28130	32.61382
0461	12:48 PM	1111	634	496,777	-117.28271	32.61271
0465_0468	12:53 PM	1170	627	507,351	-117.28431	32.61421
0474	12:57 PM	1147	610	487,636	-117.28141	32.61236
0485	1:06 PM	1257	581	509,162	-117.28209	32.61273
0489	1:11 PM	1266	595	515,862	-117.27930	32.61388
0494	1:14 PM	1250	578	490,178	-117.28360	32.61488
0501	1:18 PM	1326	592	521,542	-117.28405	32.61507
0506	1:23 PM	1405	659	592,513	-117.28321	32.61161
0511	1:27 PM	1375	738	660,168	-117.28702	32.61169
0516_0517	1:32 PM	1491	697	681,813	-117.28638	32.61160
0521	1:37 PM	1428	698	659,626	-117.28150	32.61279
0526	1:41 PM	1403	707	677,327	-117.28429	32.61325
0532	1:49 PM	1641	712	771,237	-117.28398	32.60899
0538	1:52 PM	1627	709	756,146	-117.28352	32.61155
0544	1:55 PM	1574	714	770,651	-117.28400	32.61114
0550	1:59 PM	1573	720	764,824	-117.28363	32.61333
0555_0556	2:02 PM	1775	760	843,390	-117.28348	32.60963
0560	2:06 PM	1715	720	848,430	-117.28222	32.61004
0575	2:15 PM	1768	726	843,077	-117.28040	32.61083
0583	2:21 PM	1857	683	809,878	-117.28372	32.60948
0588	2:24 PM	1821	684	818,245	-117.28249	32.60952
0592	2:27 PM	1828	697	823,571	-117.28292	32.61048
0597	2:31 PM	1778	731	845,548	-117.28217	32.61073
0605	2:34 PM	1810	705	815,648	-117.28424	32.61122
0611	2:38 PM	1808	689	808,743	-117.28294	32.61124

0621	2:46 PM	1822	750	903,684	-117.28079	32.61115
0626_0627	2:50 PM	1894	779	947,966	-117.28325	32.61022
0633	2:55 PM	1875	765	888,249	-117.27801	32.60893
0639	3:00 PM	1935	758	878,505	-117.28195	32.61169
0645_0646	3:04 PM	1972	804	981,734	-117.27817	32.61036
0653	3:09 PM	1932	795	977,203	-117.27926	32.61052
0660_0661	3:12 PM	2113	763	1,020,305	-117.27908	32.61119
0668	3:16 PM	2055	739	954,502	-117.28119	32.60693

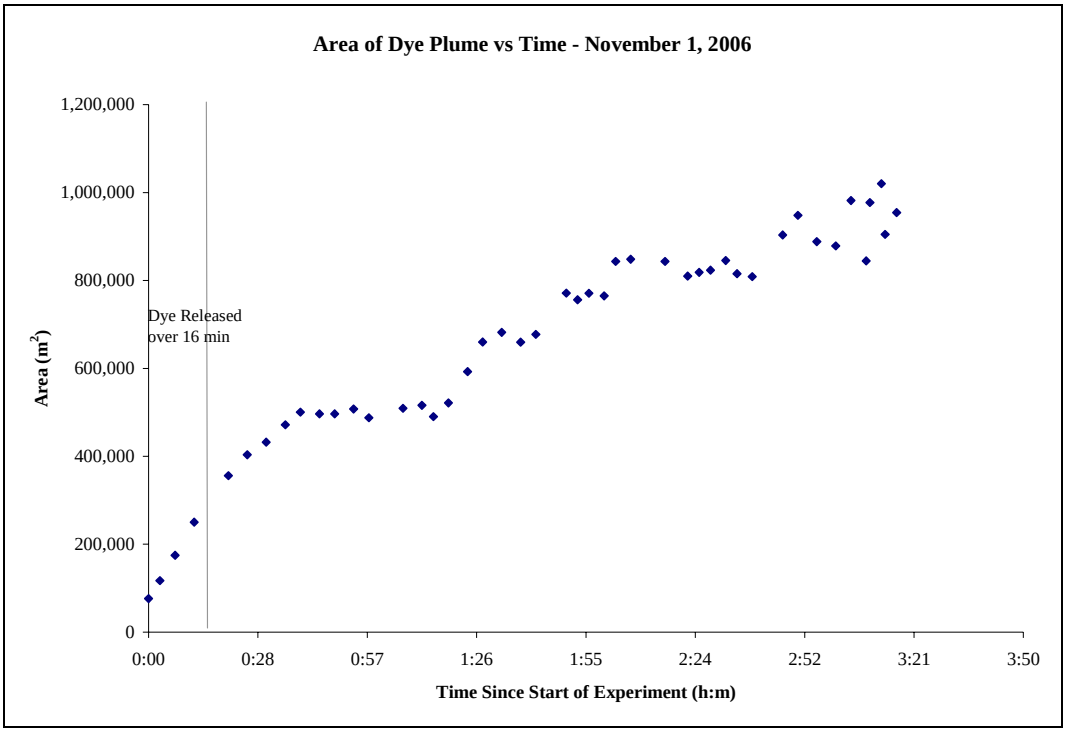

Figure B.7-5. Growth of the area of the plume, as measured from the images.

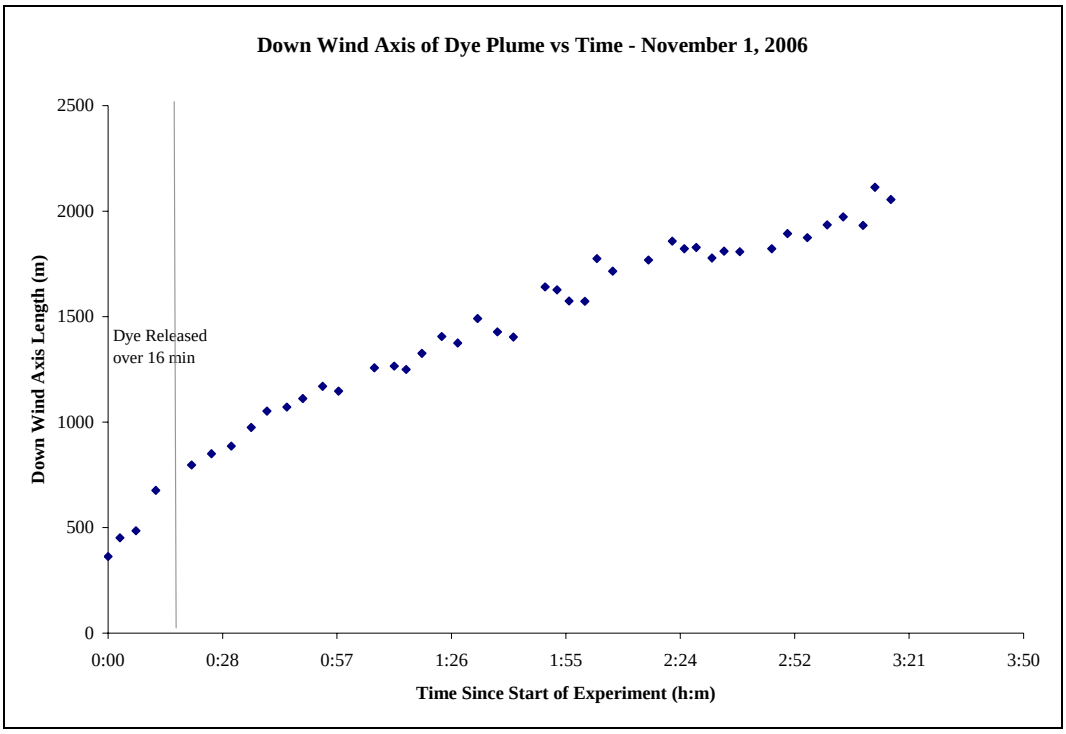

Figure B.7-6. Growth of the down-wind axis of the plume, as measured from the images.

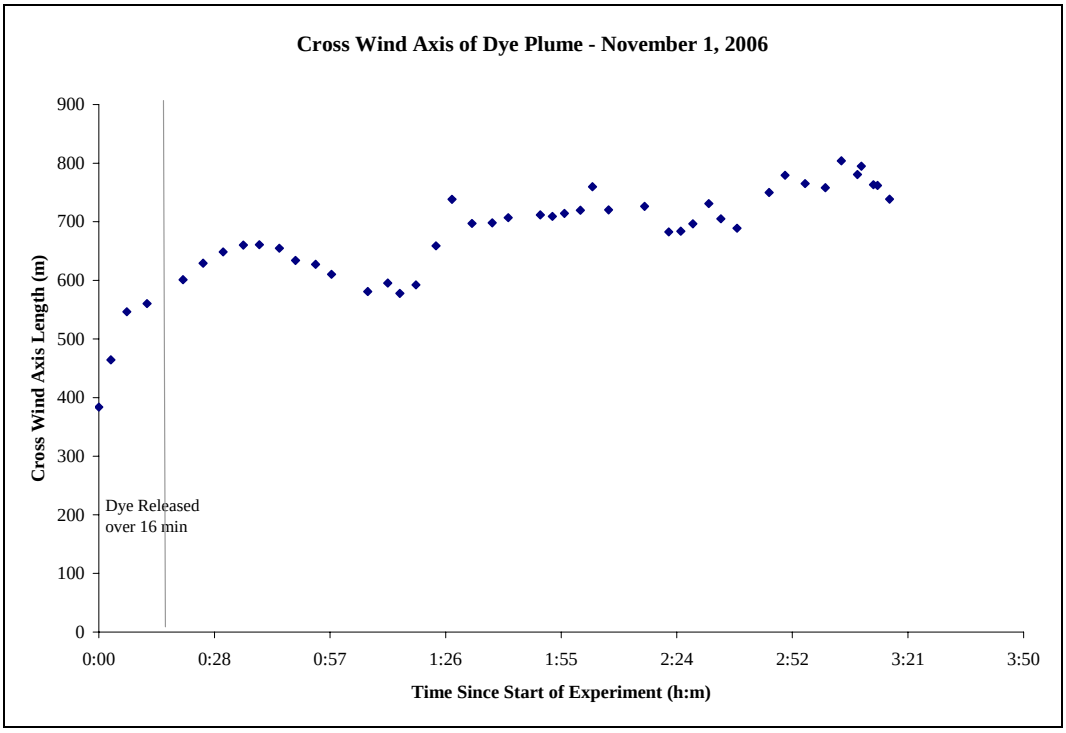

Figure B.7-7. Growth of the cross-wind axis of the plume, as measured from the images.

B.7.3 Langmuir Cell Dimensions Indicated by Dye Images

Measurements of Langmuir cell dimensions for the 1 November 2006 experiment are listed in Table B.7-3 and the means are summarized in Table B.7-4. Table B.7-5 lists the mean orientation of Langmuir cells relative to the wind direction as measured at nearly wind stations.

Table B.7-3 Measured dimensions of Langmuir circulation cells for selected images from the 1 November 2006 experiment.

Date	Image name	Time (h:m)	Time after start (h:m)	Sta. 46086 Wind dir (degrees)	Sta. 46086 Wind speed (knots)	Total width of patch in m (minor axis)	Cell orientation (degrees)	Deviation from wind direction	Major cell spacing (m)	Major cell spacing as % of patch width	Minor cell spacing (m)	Minor cell spacing as % of patch width
11/1/2006	DSC_0450	12:39	0:40	310	7.78	661	319	9	59.3	9.0	19.7	3.0
11/1/2006	DSC_0506 front	1:23	1:24	310	7.78	659	322	12	59.4	9.0	20.6	3.1
	DSC_0506 middle	1:23	1:24	310	7.78	659	319	9	80.8	12.3	N/A	N/A
	DSC_0506 back	1:23	1:24	310	7.78	659	328	18	68.7	10.4	N/A	N/A
11/1/2006	DSC_0550	1:59	2:00	310	9.72	720	321	11	58.7	8.2	34.0	4.7
11/1/2006	DSC_0605	2:34	2:35	310	9.72	705	333	23	73.8	10.5	34.2	4.9
11/1/2006	DSC_0639	3:00	3:01	310	9.72	758	336	26	74.6	9.8	36.0	4.7
	means			310	8.6	689	325	15	67.9	9.9	28.9	4.1

Table B.7-4. Mean dimensions of Langmuir circulation cells.

Date	Total width of patch in m (minor axis)	Major cell spacing (m)	Major cell spacing as % of patch width	Minor cell spacing (m)	Minor cell spacing as % of patch width
11/1/2006	689	68	10	29	4

Table B.7-5. Orientations of Langmuir circulation cells to the wind direction.

Date	Cell orientation (degrees)	Wind Station	Wind direction (degrees)	Wind speed (knots)	Deviation from wind direction
11/1/2006	325	LJPC1	325	10	0
		46086	308	9	18
		COAMPS	301	11	25

B.8 Results of November 2, 2006 Experiment

B.8.1 Movement and Spreading of Dye

The 2 November 2006 experiment began at 11:19 PST (19:19 UTC) and ended at approximately 15:00 PST (23:00 UTC). The dye plume expanded and moved primarily to the south throughout the duration of the experiment. Figure B.8-1 contains a subset of images that show the locations of the dye over time, as interpreted from the aerial photographs. In addition to the sources of georeferencing errors for images general to all experiments (Section B.1.1), in this experiment, there were additional errors due to the approximation of location data, described below.

Technical issues (i.e., suspected electronic interference/jamming by the U.S. Navy) resulted in a complete loss of all positional (altitude, location, and heading) data on the OSPR aircraft during this experiment. Through the FAA, we were able to re-obtain time-stamped positional data, which were then correlated with the time-stamps on the images. Altitude and heading information was transcribed from the hand written notes taken during the flight. Both altitude and heading are approximate values (nearest 5 degrees for heading and nearest 500 ft for altitude).

Figures B.8-1 and B.8-2(a) contain images of the dye plume over the time of the experiment, overlaid with locations of drifters, as recorded by GPS waypoints. Figure B.8-2(b) contains the same images of the dye plume over the time, with the centroids of each plotted and labeled with the time of the image. The georeferencing data located the dye shapes as displayed in Figures B.8-2(a) and B.8-2(b), displaced from the drifters to the northwest. However, as the drifters were placed in and observed to be located in the dye patch at the time of release, the dye shapes were corrected (moved in the GIS software) to overlay the initial dye location as defined by the drifter GPS measurements (Figure B.8-1). The FAA positional data placed the initial dye images about 612 m to the northwest (315^{o}, i.e., 433 m west and 433 m north) of the initial drifter locations. This appears to be a round off error in the FAA record. Thus, the dye shapes were moved 612 m in the direction of 135^{o}T (433 m east and 433 m south) before plotting in Figure B.8-1. Thus, while the dimensions of the dye plume are fairly accurate (subject to an error in altitude of up to 250 ft), the locations are only approximate.

Figures B.8-3 and B.8-4 show example georeferenced images. Figures B.8-3 and B.8-4 also show these images color coded by dye intensity (in arithmetically-scaled bins). Other images are available on the ftp site (see introduction on page 1 of Appendix B).

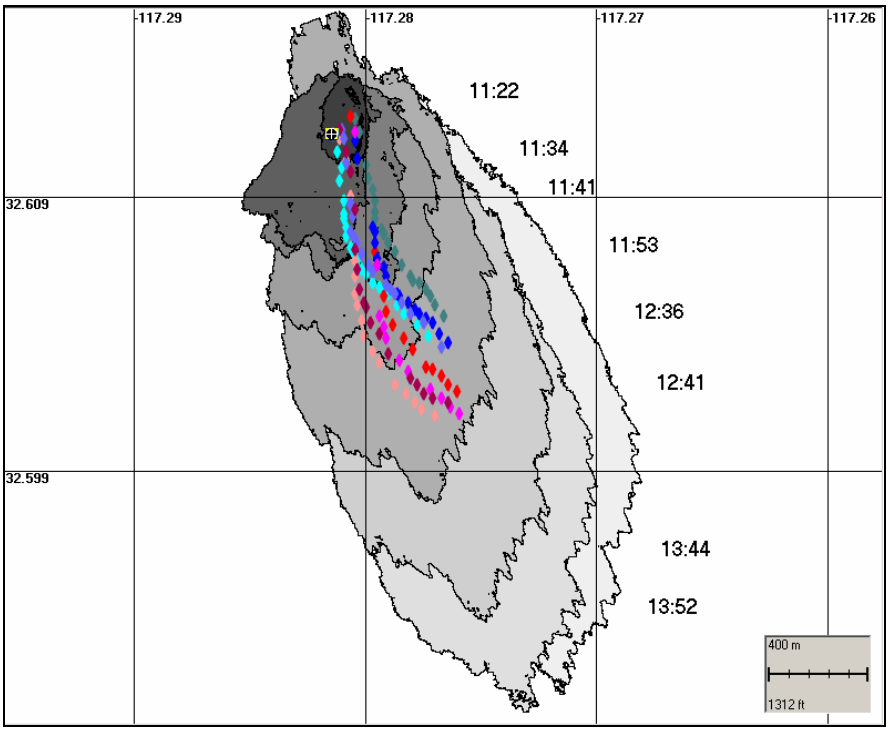

Figure B.8-1. Dye plume dimensions and movements over time, and drifter tracks represented by the diamonds (reds & purples = 2m, blues = 4m deployment depths) for the 2 November 2006 experiment.

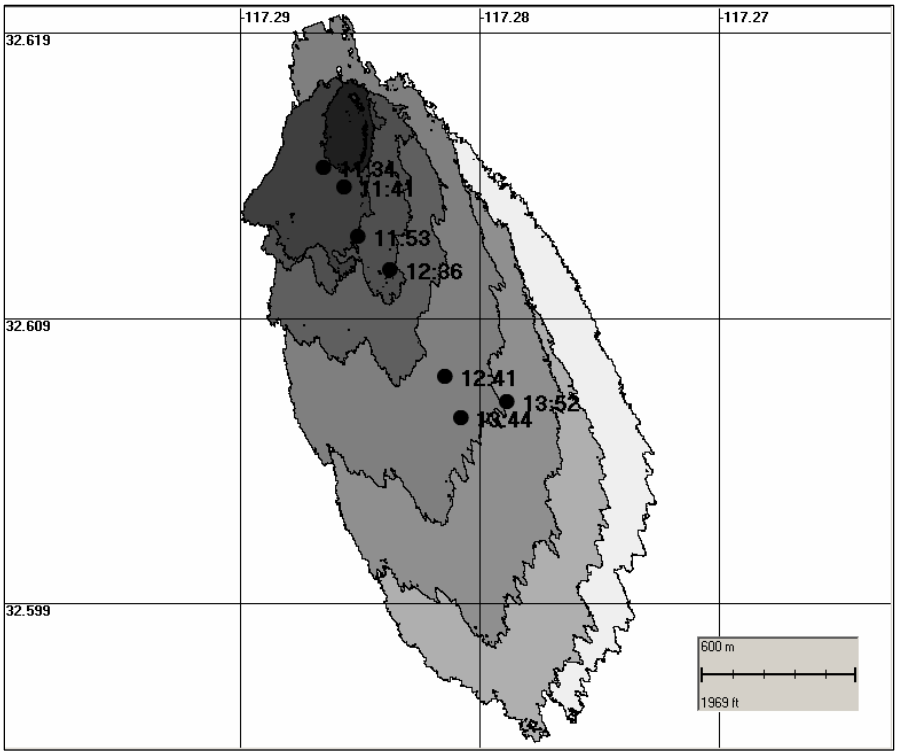

Figure B.8-2. Centroids of selected dye plume images and corresponding times on 2 November 2006).

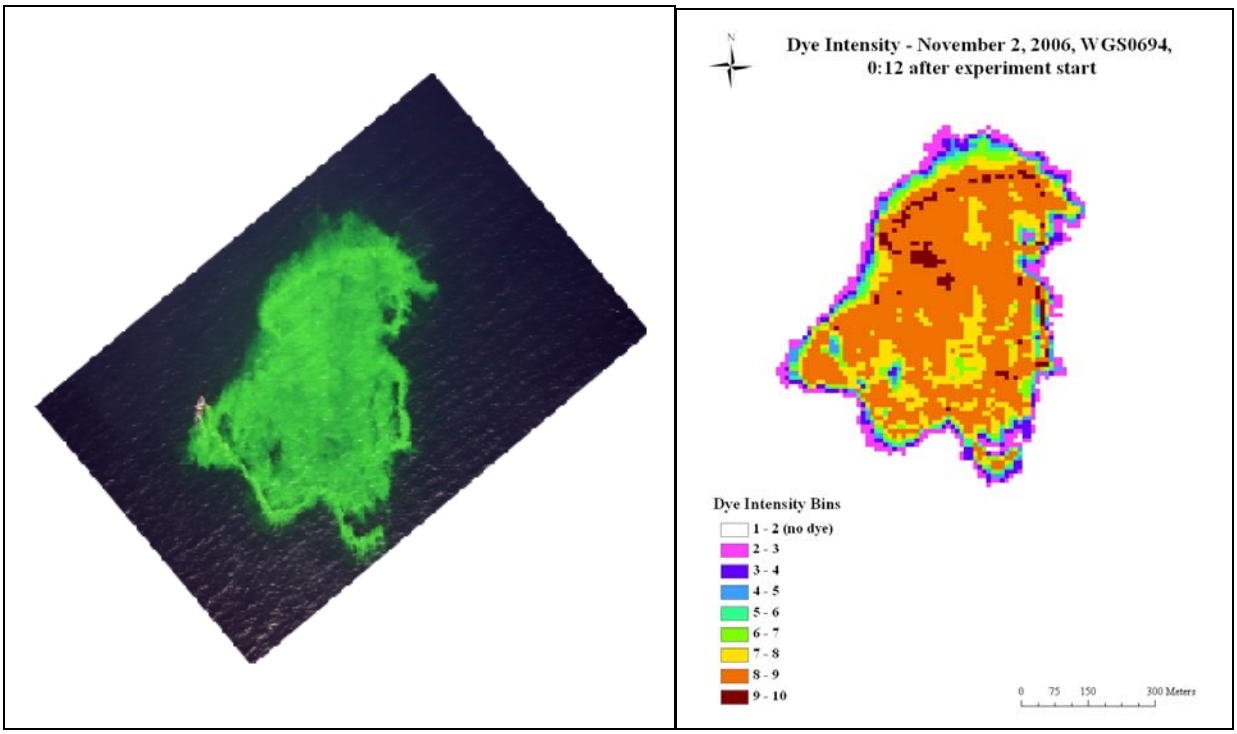

Figure B.8-3. Georectified *.tif and intensity binned (10bin) images of dye plume (image #0694, 11:34 AM on 2 November 2006).

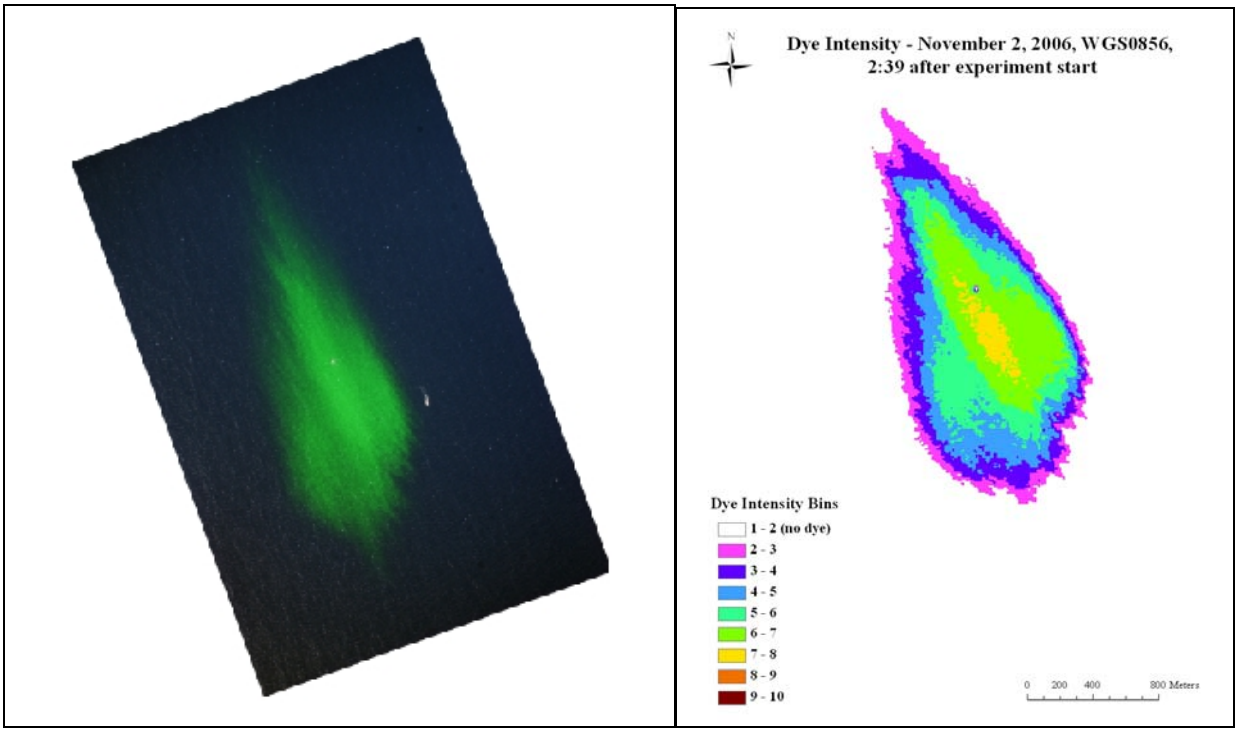

Figure B.8-4. Georectified *.tif and intensity binned (10bin) images of dye plume (image #0856, 2:01 PM on 2 November 2006).

B.8.2 Dimensions of Dye Over Time

Table B.8-1 lists the images used in the analysis of dye plume dimensions over time. The growth of the area, down-wind axis length and cross-wind axis length over time is plotted in Figures B.8-5 to B.8-7.

Table B.8-1. Data for all plume images on 2 November 2006. (Altitude data was not automatically recorded on this date – manual records of the plane's altimeter were used for estimating scale.)

Image #	Time (PST)	Down-wind axis (m)	Cross-wind axis (m)	Area (m^2)	Centroid (x)	Centroid (y)
0700	11:41 AM	850	580	337,512	-117.28558	32.61469
0704	11:45 AM	891	617	389,506	-117.28505	32.61366
0707	11:53 AM	1070	697	529,914	-117.28499	32.61287
0712	11:57 AM	1124	736	581,437	-117.28627	32.61136
0715	12:01 PM	1187	759	624,594	-117.28491	32.61315
0726	12:13 PM	1485	753	775,578	-117.28621	32.60796
0733	12:16 PM	1529	789	844,437	-117.28400	32.61297
0749	12:28 PM	1771	870	1,073,676	-117.28537	32.61182
0761	12:36 PM	1988	897	1,175,038	-117.28370	32.61170
0766	12:41 PM	2104	923	1,261,974	-117.28136	32.60791
0770	12:44 PM	2295	912	1,322,054	-117.27793	32.61135
0774	12:48 PM	2335	894	1,288,774	-117.28239	32.61396
0778	12:53 PM	2452	867	1,289,856	-117.28207	32.61520
0781	12:57 PM	2344	884	1,333,032	-117.28275	32.60950
0784	1:01 PM	2331	888	1,332,935	-117.28025	32.60878
0788	1:01 PM	2361	905	1,366,104	-117.28692	32.60731
0793	1:14 PM	2467	945	1,471,034	-117.27317	32.60924
0797	1:15 PM	2486	965	1,503,426	-117.27876	32.60647
0804	1:23 PM	2531	920	1,448,318	-117.27230	32.60880
0811	1:27 PM	2544	932	1,489,283	-117.27685	32.60996
0817	1:31 PM	2546	963	1,527,109	-117.27530	32.60867
0823	1:35 PM	2584	1011	1,584,544	-117.27659	32.60755
0828	1:39 PM	2676	1026	1,654,687	-117.27209	32.61134
0833	1:44 PM	2686	996	1,620,944	-117.28064	32.60668
0838	1:48 PM	2683	1011	1,634,065	-117.28081	32.60742
0842	1:52 PM	2615	1001	1,615,936	-117.27873	32.60700
0850	1:57 PM	2520	1021	1,680,634	-117.28548	32.61326
0856	2:01 PM	2723	1028	1,730,654	-117.28530	32.60695
0860	2:05 PM	2743	1044	1,759,818	-117.28397	32.60707
0865	2:10 PM	2838	1072	1,855,928	-117.28344	32.60999
0871	2:14 PM	2796	1078	1,876,505	-117.28630	32.60760

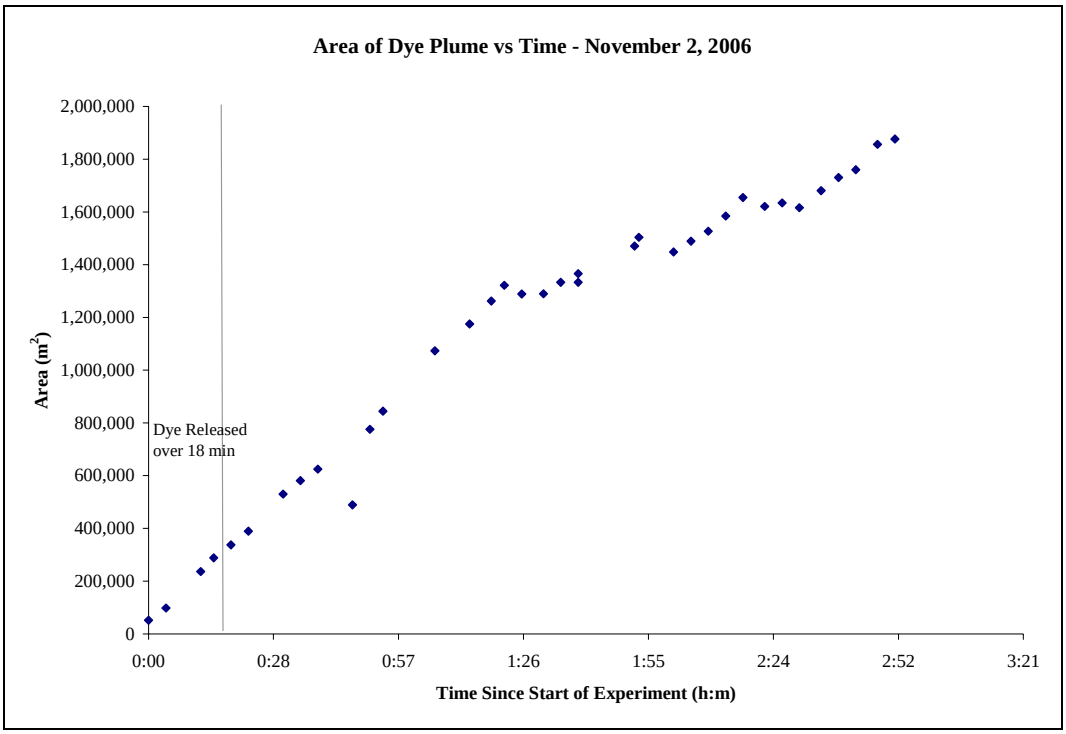

Figure B.8-5. Growth of the area of the plume, as measured from the images.

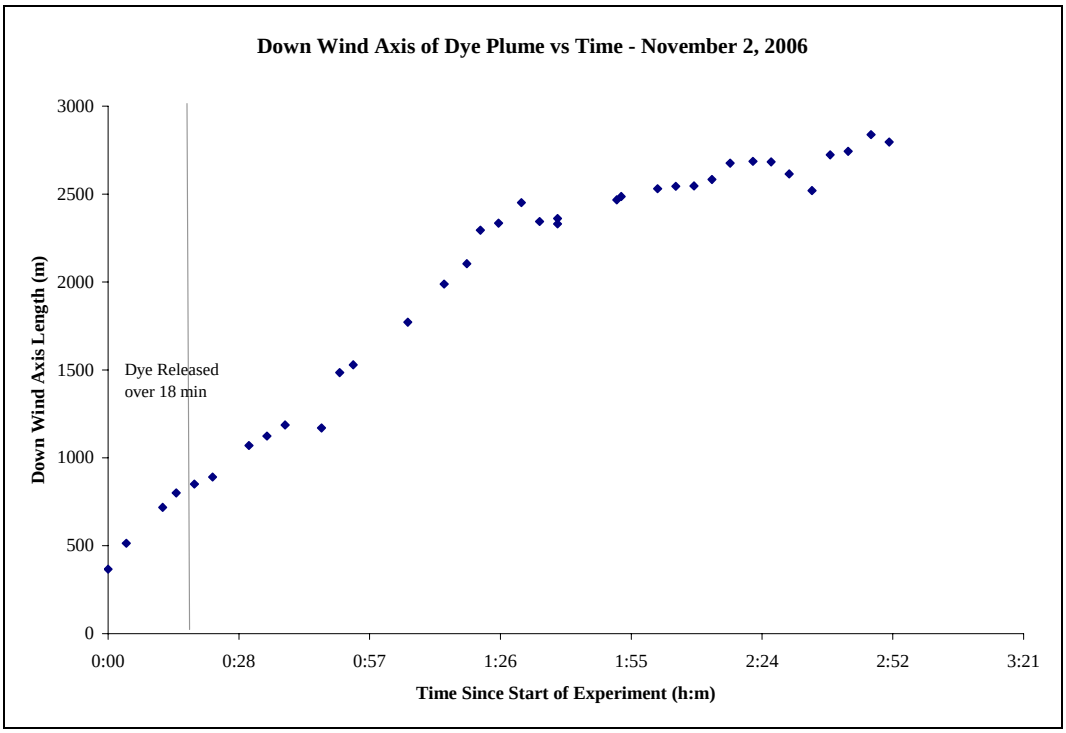

Figure B.8-6. Growth of the down-wind axis of the plume, as measured from the images.

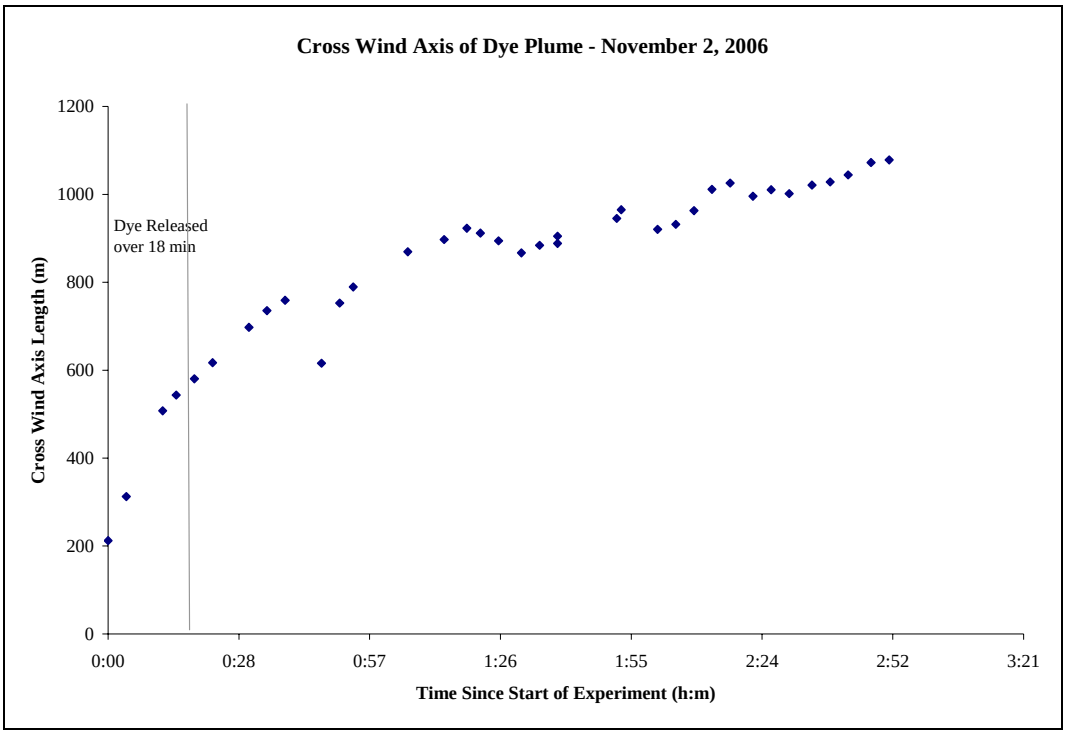

Figure B.8-7. Growth of the cross-wind axis of the plume, as measured from the images.

B.8.3 Langmuir Cell Dimensions Indicated by Dye Images

Measurements of Langmuir cell dimensions for the 2 November 2006 experiment are listed in Table B.8-2 and the means are summarized in Table B.8-3. Table B.8-4 lists the mean orientation of Langmuir cells relative to the wind direction as measured at nearby wind stations.

Table B.8-2 Measured dimensions of Langmuir circulation cells for selected images from the 2 November 2006 experiment.

Date	Image name	Time (h:m)	Time after start (h:m)	Sta. 46086 Wind dir (degrees)	Sta. 46086 Wind speed (knots)	Total width of patch in m (minor axis)	Cell orientation (degrees)	Deviation from wind direction	Major cell spacing (m)	Major cell spacing as % of patch width	Minor cell spacing (m)	Minor cell spacing as % of patch width
11/2/2006	DSC_0704	11:45	0:23	320	11.66	616	334	14	26.9	4.4	N/A	N/A
11/2/2006	DSC_0715	12:01	0:39	320	11.66	758	335	15	43.1	5.7	15.4	2.0
11/2/2006	DSC_0811	13:27	2:05	330	11.66	931	324	-6	35.7	3.8	N/A	N/A
11/2/2006	DSC_0871	14:14	2:52	330	13.61	1078	328	-2	52.9	4.9	N/A	N/A
	means			325	12.1	846	330	5	39.6	4.7	15.4	2.0

Table B.8-3. Mean dimensions of Langmuir circulation cells.

Date	Total width of patch in m (minor axis)	Major cell spacing (m)	Major cell spacing as % of patch width	Minor cell spacing (m)	Minor cell spacing as % of patch width
11/2/2006	846	40	5	15	2

Table B.8-4. Orientations of Langmuir circulation cells to the wind direction.

Date	Cell orientation (degrees)	Wind Station	Wind direction (degrees)	Wind speed (knots)	Deviation from wind direction
11/2/2006	330	LJPC1	338	8	-7
		46086	325	12	5
		COAMPS	318	11	12

B.9 Results of August 9, 2006 Safe Seas Experiment

B.9.1 Movement and Spreading of Dye

The 9 August 2006 dye release began at 11:50 PDT (19:50 UTC) and was tracked until approximately 13:30 PDT (20:30 UTC) when the dye became too diffuse to effectively photograph. Unfortunately, the dye was not released in a focused circular area, instead being released from a hose in a curvilinear manner in generally a cross-wind direction (Figure B.9-1). This made analysis of the dye dimensions difficult, and any data resulting from such an analysis would be difficult or impossible to interpret. Such interpretation was not attempted, both for this reason and because of the lack of drifter data in the area of the dye release.

Selected images of the dye movements for this experiment (which were the most complete image at each overpass of the plane taking the photographs) are listed in Table B.9-1 and shown in Figure B.9-2. The dye patch moved northward until the last image at 13:27 hours. In addition to the sources of georeferencing errors for images general to all experiments (Section B.1.1), in this experiment, there were additional errors due to the approximation of location data, as is evident in the images. However, the trajectory of the dye patch may be determined from the image movements.

Table B.9-1 Selected images from the 9 August 2006 Safe Seas experiment.

Image #	Time (PDT)	Longitude (degrees W)	Latitude (degrees N)
Dsc_0019.jpg	11:54	-122.61412	37.66123
Dsc_0088.jpg	12:34	-122.61391	37.66513
Dsc_0096.jpg	12:39	-122.61323	37.66543
Dsc_0106.jpg + Dsc_0107.jpg	12:44	-122.61353	37.66585
Dsc_0115.jpg + Dsc_0116.jpg	12:48	-122.61245	37.66682
Dsc_0127.jpg + Dsc_0128.jpg	12:53	-122.61274	37.66701
Dsc_0134.jpg + Dsc_0135.jpg	12:58	-122.61195	37.66748
Dsc_0143.jpg + Dsc_0144.jpg + Dsc_0145.jpg	13:02	-122.61203	37.66695
Dsc_0157.jpg	13:11	-122.60923	37.66704
Dsc_0181.jpg	13:18	-122.61023	37.66801
Dsc_0214.jpg	13:27	-122.60687	37.66681

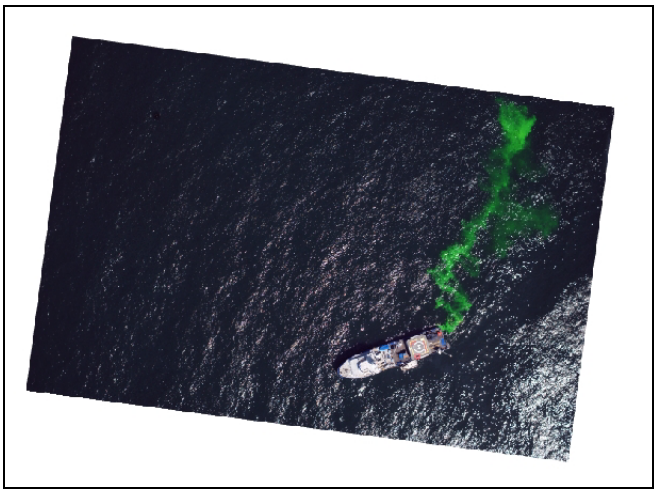

Figure B.9-1. Georectified *.tif image of dye plume (image #0019, 11:54 AM on 9 August 2006).

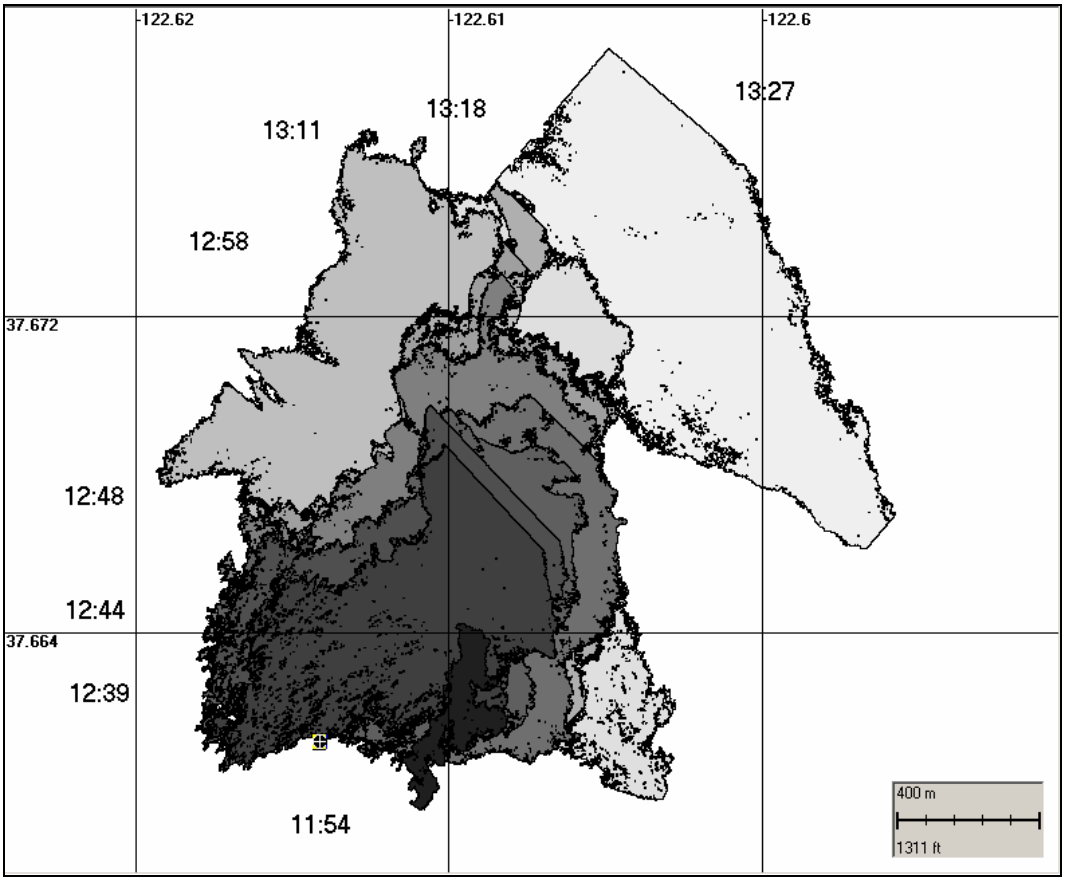

Figure B.9-2. Dye plume dimensions and movements over time for the 9 August 2006 experiment.